



**HAL**  
open science

## Validation of ozone measurements from the Improved Limb Atmospheric Spectrometer

T. Sugita, T. Yokota, H. Nakajima, H. Kanzawa, H. Nakane, H. Gernandt, V. Yushkov, K. Shibasaki, T. Deshler, Y. Kondo, et al.

► **To cite this version:**

T. Sugita, T. Yokota, H. Nakajima, H. Kanzawa, H. Nakane, et al.. Validation of ozone measurements from the Improved Limb Atmospheric Spectrometer. *Journal of Geophysical Research: Atmospheres*, 2002, 107 (D24), pp.ILS 9-1-ILS 9-22. 10.1029/2001JD000602 . insu-03039698

**HAL Id: insu-03039698**

**<https://insu.hal.science/insu-03039698>**

Submitted on 4 Dec 2020

**HAL** is a multi-disciplinary open access archive for the deposit and dissemination of scientific research documents, whether they are published or not. The documents may come from teaching and research institutions in France or abroad, or from public or private research centers.

L'archive ouverte pluridisciplinaire **HAL**, est destinée au dépôt et à la diffusion de documents scientifiques de niveau recherche, publiés ou non, émanant des établissements d'enseignement et de recherche français ou étrangers, des laboratoires publics ou privés.

## Validation of ozone measurements from the Improved Limb Atmospheric Spectrometer

T. Sugita,<sup>1</sup> T. Yokota,<sup>1</sup> H. Nakajima,<sup>1</sup> H. Kanzawa,<sup>1</sup> H. Nakane,<sup>1</sup> H. Gernandt,<sup>2</sup> V. Yushkov,<sup>3</sup> K. Shibasaki,<sup>4</sup> T. Deshler,<sup>5</sup> Y. Kondo,<sup>6</sup> S. Godin,<sup>7</sup> F. Goutail,<sup>7</sup> J.-P. Pommereau,<sup>7</sup> C. Camy-Peyret,<sup>8</sup> S. Payan,<sup>8</sup> P. Jeseck,<sup>8</sup> J.-B. Renard,<sup>9</sup> H. Bösch,<sup>10</sup> R. Fitzenberger,<sup>10</sup> K. Pfeilsticker,<sup>10</sup> M. von König,<sup>11</sup> H. Bremer,<sup>11</sup> H. Küllmann,<sup>11</sup> H. Schlager,<sup>12</sup> J. J. Margitan,<sup>13</sup> B. Stachnik,<sup>13</sup> G. C. Toon,<sup>13</sup> K. Jucks,<sup>14</sup> W. A. Traub,<sup>14</sup> D. G. Johnson,<sup>14,15</sup> I. Murata,<sup>16</sup> H. Fukunishi,<sup>16</sup> and Y. Sasano<sup>1</sup>

Received 7 March 2001; revised 11 July 2001; accepted 16 July 2001; published 19 October 2002.

[1] Vertical profiles of ozone concentration in the high latitudes were observed by the Improved Limb Atmospheric Spectrometer (ILAS) aboard the Advanced Earth Observing Satellite (ADEOS) from November 1996 to June 1997. The ozone data obtained by the version 5.20 ILAS retrieval algorithm are compared with those obtained by the version 19 Halogen Occultation Experiment (HALOE), the version 6 Stratospheric Aerosol and Gas Experiment (SAGE) II, and the version 6 Polar Ozone and Aerosol Measurement (POAM) II retrieval algorithms. The ILAS data are also compared with ozone data measured by ozonesondes, instruments on board balloons or an aircraft, and ground-based instruments. The ILAS ozone data generally agree with its correlative data between 11 and 64 km with some exceptions. Quantitatively, the median value of the relative difference (absolute difference divided by its mean value) for these comparisons was within  $\pm 10\%$ . Relative differences (18%) exceeding the combined measurement errors were found around 45–55 km altitude from comparisons with the HALOE and SAGE II data in January 1997 in the Southern Hemisphere (SH). Larger relative differences (around 50%) were also found below 15 km from comparisons with the HALOE and POAM II data in November 1996 in the SH, but these absolute differences were 0.10–0.16 ppmv as the median value. The ozone data processed by the version 5.20 were improved compared to the former version 3.10, which is available to the general public. The version 5.20 ozone data can be used for scientific analysis purposes based on the accuracy of the data in comparison with these other instruments. *INDEX TERMS*: 0340 Atmospheric Composition and Structure: Middle atmosphere—composition and chemistry; 0341 Atmospheric Composition and Structure: Middle atmosphere—constituent transport and chemistry (3334); 3360 Meteorology and Atmospheric Dynamics: Remote sensing; *KEYWORDS*: ILAS, solar occultation, stratosphere, ozone

**Citation:** Sugita, T., et al., Validation of ozone measurements from the Improved Limb Atmospheric Spectrometer, *J. Geophys. Res.*, 107(D24), 8212, doi:10.1029/2001JD000602, 2002.

<sup>1</sup>Ozone Layer Research Project, National Institute for Environmental Studies, Tsukuba, Ibaraki, Japan.

<sup>2</sup>Alfred Wegener Institute for Polar and Marine Research, Bremerhaven, Germany.

<sup>3</sup>Central Aerological Observatory, Dolgoprudny, Russia.

<sup>4</sup>Faculty of Letters, Kokugakuin University, Tokyo, Japan.

<sup>5</sup>Department of Atmospheric Science, University of Wyoming, Laramie, Wyoming, USA.

<sup>6</sup>Research Center for Advanced Science and Technology, University of Tokyo, Tokyo, Japan.

<sup>7</sup>Service d'Aéronomie, CNRS, Paris, France.

<sup>8</sup>Laboratoire de Physique Moléculaire et Applications, CNRS, Paris, France.

<sup>9</sup>Laboratoire de Physique et Chimie de l'Environnement, CNRS, Orléans, France.

<sup>10</sup>Institut für Umweltphysik, University of Heidelberg, Heidelberg, Germany.

<sup>11</sup>Institut für Umweltphysik, University of Bremen, Bremen, Germany.

<sup>12</sup>Institut für Physik der Atmosphäre, DLR, Oberpfaffenhofen, Germany.

<sup>13</sup>Jet Propulsion Laboratory, California Institute of Technology, Pasadena, California, USA.

<sup>14</sup>Harvard-Smithsonian Center for Astrophysics, Cambridge, Massachusetts, USA.

<sup>15</sup>Now at NASA Langley Research Center, Hampton, Virginia, USA.

<sup>16</sup>Department of Geophysics, Tohoku University, Sendai, Japan.

## 1. Introduction

[2] It is essential to monitor and understand current trends in the vertical distribution of ozone in order to predict its future trends. The abundance of ozone in the upper troposphere and stratosphere plays an important role not only in photochemical processes [e.g., *WMO*, 1999] but also in radiative forcing [e.g., *Shine and Forster*, 1999]. The trends for 1979–1996 have recently been assessed by an international scientific joint project, utilizing long-term quality controlled ozonesonde data, ground-based data, and satellite data [*WMO*, 1998]. The trend in the upper stratosphere can be interpreted as being the result of increasing anthropogenic chlorine emissions; photochemical model calculations closely reproduce it [*WMO*, 1999]. However, understanding the trend in the lower stratosphere is more complicated, because the abundance of lower stratospheric ozone is mainly dominated by transport processes [e.g., *WMO*, 1986]. The abundance is also dependent on the abundances of reactive hydrogen, nitrogen, and halogen directly through gas phase chemistry [e.g., *Wennberg et al.*, 1994], which are regulated through heterogeneous reactions occurring on/in stratospheric sulfate aerosols [e.g., *Hofmann and Solomon*, 1989] and/or polar stratospheric clouds (PSCs) [e.g., *Solomon et al.*, 1986]. It could be also related to the degree of stratospheric denitrification in the spring time polar vortices [e.g., *Tabazadeh et al.*, 2000; *Waibel et al.*, 1999].

[3] One of the important data sources for monitoring the trends in the vertical distribution of ozone is data from the Stratospheric Aerosol and Gas Experiment (SAGE) I and II measurements [e.g., *Randel et al.*, 1999]. The SAGE instruments make use of the solar occultation technique, which is capable of relatively high vertical resolution measurements for a satellite instrument with high accuracy and precision. However, since SAGE I and II were put into a processing orbit, they can not measure the vertical distribution of ozone in the high latitudes continuously. In order to monitor the changes in stratospheric ozone distribution in the high latitudes, the Improved Limb Atmospheric Spectrometer (ILAS), which also makes use of the solar occultation technique, aboard the Advanced Earth Observing Satellite (ADEOS) was launched from Tanegashima island, Japan (30°N, 131°E) in August 1996. Until 30 June 1997, when the ADEOS stopped working due to a solar paddle array failure, about 5800 vertical profiles of ozone concentration were successfully retrieved [*Sasano et al.*, 1999b]. The measurement period of ILAS filled a gap in the Polar Ozone and Aerosol Measurement (POAM) II and III measurement periods (October 1993 to November 1996 for POAM II and April 1998 to the present for POAM III) [*Bevilacqua*, 1997; *Lucke et al.*, 1999]. POAM also makes use of the solar occultation technique.

[4] The ILAS ozone data processed by the version 3.10 retrieval algorithm have been compared with version 18 Halogen Occultation Experiment (HALOE) ozone data [*Lee et al.*, 1999]. It was shown that the ILAS data are 13% smaller than the HALOE data between 20 and 40 km for the Northern Hemisphere (NH) and 20% smaller than those in the Southern Hemisphere (SH). Comparisons with ozonesonde measurements at 5 stations indicate that the version 3.10 ILAS ozone data have an accuracy better than 20% between 20 and 35 km [*Sasano et al.*, 1999a]. Since these

validation papers, using version 3.10 products, were published, the retrieval algorithm has been updated by introducing an altitude registration method developed by *Nakajima et al.* [2002b].

[5] This paper focuses on an assessment of the quality of the ILAS ozone data processed by the latest retrieval algorithm, version 5.20, through comparisons with many coincident measurements. During the ILAS measurement period, November 1996 to June 1997, three satellite-borne solar occultation sensors were operated: SAGE II [*Mauldin et al.*, 1985] and the HALOE [*Russell et al.*, 1993] which have been operating since 1984 and 1991, respectively, and POAM II [*Glaccum et al.*, 1996] which operated from 1993 to November 1996. We used these three data sets for validating the ILAS data. In addition, data obtained by ozonesondes launched from 13 stations in the NH and 3 stations in the SH as well as data obtained by remote sensing or in situ sensors from balloon, aircraft, or ground during the ADEOS/ILAS validation campaign conducted in Kiruna, Sweden (68°N, 21°E) and Fairbanks, Alaska (65°N, 148°W) [*Kanzawa et al.*, 1997] are also used.

## 2. Instrumentation and Data Sets

### 2.1. ILAS

[6] ILAS is a solar occultation sensor which consists of two grating spectrometers (covering 6.21–11.77  $\mu\text{m}$  with a 44-spectral element pyroelectric array detector and 0.753–0.784  $\mu\text{m}$  with a 1024-spectral element metal oxide semiconductor (MOS) photodiode array detector, respectively) and a Sun edge sensor [*Nakajima et al.*, 2002a; *Sasano et al.*, 1999a, 1999b]. A brief description of the ILAS characteristics and the retrieval algorithm version used here are listed in the left column of Table 1. The  $\nu_3$  band centered near 9.6  $\mu\text{m}$  is used for detecting ozone molecules. The instantaneous field of view (IFOV) at tangent height (TH) has a 1.6 km width in the vertical and a 13 km width in the horizontal direction for the infrared (IR) spectrometer. The partial slant path along the line of sight within a 1 km thick layer just above the TH of 20 km is less than 230 km. With a sampling rate of 12 Hz, a full spectrum over the 44 IR spectral elements is acquired within 0.88 ms, i.e., one major frame is corresponding to about 110 m at the TH of 15 km and 270 m at the TH of 55 km, depending on atmospheric refraction. Time series smoothing, which corresponds to about 10 major frames, is applied in the transmittance data, so the actual vertical resolution is 1.9 km at the TH of 15 km and 3.5 km at the TH of 55 km [*Yokota et al.*, 2002]. For reference, the vertical resolution is estimated to be  $\sim 1$ ,  $\sim 2$ , and 1–1.5 km for SAGE II, HALOE, and POAM II instruments, respectively, as listed in Table 1. The ADEOS satellite was put into a Sun-synchronous polar orbit. The inclination angle of ADEOS is 98.6°, and the equator crossing time is around 1040 local mean solar time (descending). Therefore, the ILAS occultation event occurred at sunrise and sunset seen from the ADEOS satellite on each of about 14 orbits per 24 hours. The measurement region of the ILAS is over high latitude (57–70°N and 64–88°S), as shown in Figure 1.

[7] Vertical profiling of atmospheric constituents is performed by using an “onion-peeling” method [*Yokota et al.*, 2002]. The retrieved altitude for ozone ranges from 8 km (at

**Table 1.** A Summary of Each Sensor Used in This Analysis

	ILAS <sup>a</sup>	SAGE II <sup>b</sup>	HALOE <sup>c</sup>	POAM II <sup>d</sup>
Instrumentation	grating spectrometer	Sun photometer	broadband radiometer	Sun photometer
O <sub>3</sub> detection wavelength	$\nu_3$ band <sup>e</sup>	600 nm	$\nu_3$ band <sup>f</sup>	601 nm
I FOV in vertical (km)	1.6	0.5	1.6	0.8
Vertical resolution (km)	2–3.5	~1	~2	1–1.5
Sampling rate (Hz)	12	64	8	18
Data grid of geometric altitude (km)	1	0.5	0.3	1
Altitude registration uncertainty (m)	$300 \pm 360^g$	250 <sup>h</sup>	150 <sup>i</sup>	200 <sup>j</sup>
Algorithm version	5.20	6	19	6

<sup>a</sup>Nakajima *et al.* [2002a].<sup>b</sup>Mauldin *et al.* [1985].<sup>c</sup>Russell *et al.* [1993].<sup>d</sup>Glaccum *et al.* [1996].<sup>e</sup>The range of the 16 grating spectrometer elements covering the O<sub>3</sub> band is 978–1189 cm<sup>-1</sup>.<sup>f</sup>The range of the wideband filter covering the O<sub>3</sub> band is 960–1080 cm<sup>-1</sup>.<sup>g</sup>Nakajima *et al.* [2002b].<sup>h</sup>Cunnold *et al.* [2000].<sup>i</sup>Brühl *et al.* [1996].<sup>j</sup>Lumpe *et al.* [1997].

the lowest) to 70 km. A summary of error analysis for the version 5.20 ILAS ozone data is shown in Tables 2 and 3. The error values of the version 5.20 data are sorted into “internal” and “external.” “Internal” errors refer to errors calculated from the final residuals after convergence of the nonlinear least squares fitting for observed and simulated transmittances. “External” errors refer to errors associated with the calculation of simulated transmittance through uncertainties in the nongaseous component correction and temperature profiles, which are used as inputs for the retrieval.

[8] The nongaseous component correction [Sasano *et al.*, 1999b; Yokota *et al.*, 2002] is required in order to derive vertical profiles of the gaseous concentration in the altitude range where extinction due to aerosol particles (sulfate aerosols and/or PSCs) can not be neglected. To determine the nongaseous component in the simulated transmittance, we first evaluate the optical depth due to the gaseous component at the 4 spectral elements where the absorption due to gaseous species is relatively small (so-called window spectral element). To do so, we use profiles for ozone, HNO<sub>3</sub>, NO<sub>2</sub>, N<sub>2</sub>O, H<sub>2</sub>O, CH<sub>4</sub>, CO<sub>2</sub>, and other minor gaseous concentrations (such as CFC-11) from an ILAS reference atmosphere model [Yokota *et al.*, 2002]. Then, the nonaerosol (i.e., gaseous only) optical depth at all the other 40 spectral elements is calculated by linear interpolation between these 4 window spectral elements. Use of data from this reference atmosphere model would make some errors for the calculation of simulated transmittance. The magnitude of these errors has been estimated from simulations by using 10 percentile, median, and 90 percentile in these reference data. These errors are one of the components of the external errors. The interpolation would also produce systematic errors for the retrieved profiles of the gaseous concentration, but we do not include it to the external error. We will evaluate the corresponding uncertainty later in this subsection.

[9] Effects from uncertainties of temperature, which are used in the calculation of simulated transmittance, are also included (the uncertainties of  $\pm 2$  K at 10 km altitude and  $\pm 5$  K at 70 km altitude are assumed). A detailed description of error analysis is given by Yokota *et al.* [2002]. The estimated root-sum-square (RSS) total uncertainties (internal + external errors) in ozone mixing ratio values have been converted in percent errors by using an average ozone value

(obtained as the average of all version 5.20 ozone retrievals). The average error then amounts to 14, 9, 3, 3, 4, and 7% at 15, 20, 30, 40, 50, and 60 km, respectively, as listed in Table 2. We used this total uncertainty provided in each version 5.20 ILAS data file. In addition, the relative standard deviation (RSD) was calculated as one sigma standard deviation (around the mean) divided by the mean value over quiescent periods (3–5 days at the end of March 1997 in the SH or June 1997 in the NH). This quantity includes a measure of geophysical variability and repeatability of the measurement. The RSD was observed to be smaller than the RSS total error defined above [see also Yokota *et al.*, 2002].

[10] Two points should be noted in terms of uncertainties in the retrieved profiles. First, it is crucial whether TH is determined accurately or not, because TH ambiguity propagates directly to the uncertainty in retrieving volume mixing ratio profiles. For the version 3.10 algorithm, a tentative method for determining the TH was used, as described by Sasano *et al.* [1999b]. For the version 5.20 algorithm, the TH was determined with a method discussed by Nakajima *et al.* [2002b]. The estimated uncertainty in the altitude registration for the tangent point is  $300 \pm 360$  m. For reference, the uncertainties in altitude registration are estimated to be 250, 150, and 200 m for SAGE II, HALOE, and POAM II instruments, respectively, as listed in Table 1.

[11] The second point is systematic errors associated with the nongaseous component correction. To evaluate systematic errors caused by the simple linear interpolation between the window spectral elements, we simulated transmittances using several types of IR absorption spectra for sulfate aerosols (50 and 75 wt % H<sub>2</sub>SO<sub>4</sub>/H<sub>2</sub>O binary solutions) and PSCs (nitric acid trihydrate (NAT), supercooled ternary solutions (STS) for four compositions, and ice) as the nongaseous component and the above mentioned reference profiles (a priori profiles) as the gaseous component [Yokota *et al.*, 2002]. Using these simulated transmittances, retrievals of the vertical profile of the gaseous concentration were made after applying the linear interpolation method for the nongaseous contribution in the version 5.20 retrieval algorithm discussed here. The difference between a priori and the retrieved ozone profiles expressed in number density were well correlated with aerosol extinction coefficient (AEC) at 780 nm. Therefore, we can evaluate the systematic errors in

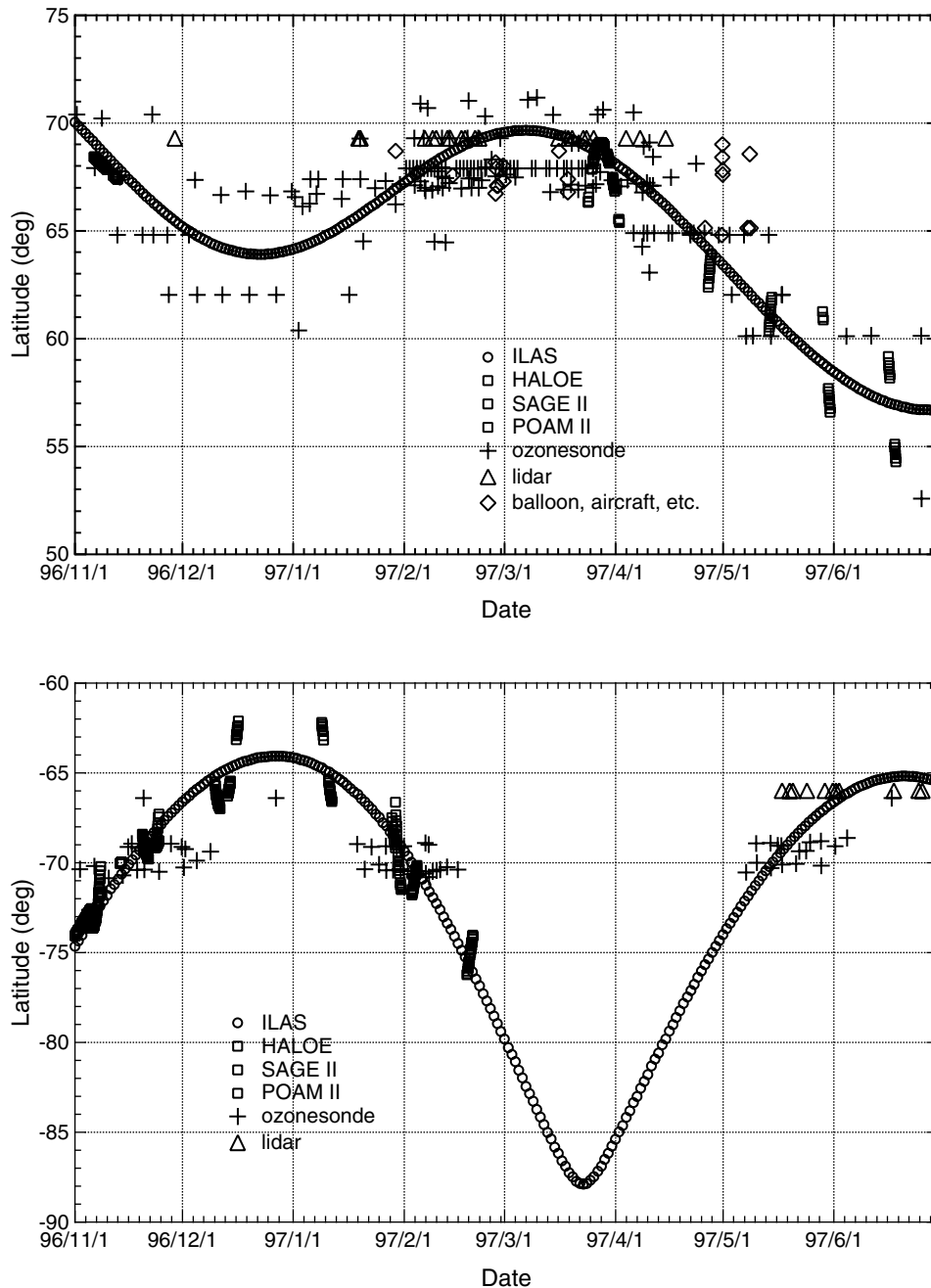


**Figure 1.** Latitudinal coverage of ILAS and the coincident measurements from SAGE II, HALOE, POAM II, ozonesondes, balloon-borne, airborne, and ground-based instruments. The upper panel shows the NH and the bottom panel shows the SH. See color version of this figure at back of this issue.

ozone number density as a function of the AEC at 780 nm. Assuming typical air number densities at altitudes of 15, 20, and 25 km, the errors on volume mixing ratio values ranged from  $-0.06$  to  $0.15$  ppmv for the two types of sulfate aerosol with a value of the AEC of  $5 \times 10^{-4} \text{ km}^{-1}$ , as listed in Table 3. These systematic biases for the several types of PSCs are also listed in Table 3. A detailed description of this error analysis is given by Yokota *et al.* [2002].

**2.2. SAGE II, HALOE, and POAM II**

[12] Table 1 also outlines the characteristics of the SAGE II, HALOE, and POAM II instruments. In this analysis, we

used data processed by version 6, 19, and 6 retrieval algorithms for SAGE II, HALOE, and POAM II, respectively. All of the data are available for scientific use through their World Wide Web servers. For version 6 SAGE II data, the error for the ozone data has been significantly reduced, reaching 2.5% accuracy [Manney *et al.*, 2001]. For error values of the SAGE II ozone data, we used a RSS combining this level of accuracy and the random error described in each SAGE II data file. Estimated RSS total errors for the version 17 HALOE ozone are 8, 12, and 30% at 1, 10, and 100 hPa, respectively, as listed by Brihl *et al.* [1996, Table 1]. For error values of the version 19 HALOE ozone

**Table 2.** A Summary of Error Analysis for the Version 5.20 Ozone Data, Part 1

Altitude, km	Meas. Rep., %	Internal, <sup>a</sup> ppmv	External, ppmv	Average, <sup>b</sup> ppmv	Total RSS, <sup>c</sup> %
9	19	0.15	0.12	0.20	98
12	11	0.09	0.07	0.46	25
15	7	0.13	0.07	1.09	14
20	3	0.22	0.14	2.91	9
25	4	0.18	0.10	4.16	5
30	2	0.14	0.03	5.06	3
35	2	0.17	<0.01	5.74	3
40	2	0.14	<0.01	5.10	3
45	2	0.10	<0.01	3.49	3
50	3	0.09	<0.01	2.35	4
55	3	0.08	<0.01	1.50	5
60	4	0.06	<0.01	0.84	7

<sup>a</sup>Average of internal errors associated with all retrievals.<sup>b</sup>Average of all retrievals.<sup>c</sup>RSS of internal and external errors divided by average.

data, we used the RSS of errors associated with the aerosol effects, which are described in each HALOE data file, and errors given by *Brühl et al.* [1996, Table 1] except for errors associated with the aerosol effects (J. M. Russell III, private communication, 2000). The random and systematic errors in the version 5 POAM II retrievals are both around 5% between 10 and 50 km [*Lumpe et al.*, 1997]. For error values of the version 6 POAM II ozone data, we used the RSS of the random error described in each POAM II data file and the systematic error of 5%. A comparative study of ozone profiles measured by seven satellite instruments including the version 6 SAGE II, the version 19 HALOE, and the version 6 POAM II data was made by *Manney et al.* [2001]. The results suggest that ozone data generally agree to within  $\sim 0.25$  and 0.5 ppmv between each other in the lower and upper stratosphere, respectively.

### 2.3. Ozonesondes

[13] Ozonesonde data that have been registered in two databases are used here; one is the ILAS Correlative Measurement Database (CMDB) at the National Institute for Environmental Studies (NIES) and the other is the Ozone Soundings as a tool for Detecting Ozone Change (OSDOC) database at the Norwegian Institute for Air Research (NILU). In the former database, data obtained mainly through the ADEOS/ILAS validation campaign conducted in Kiruna, Sweden (68°N, 21°E) and Fairbanks, Alaska (65°N, 148°W) have been registered [*Kanzawa et al.*, 1997]. The latter database is dedicated to studies such as Lagrangian ozone loss rate calculations using the “Match” technique

[e.g., *Schulz et al.*, 2000]. The data from Kiruna and Yakutsk stations have been registered in both databases. Along with these two databases, we used ozonesonde data from Fairbanks, which has been registered in the POLARIS (Photochemistry of Ozone Loss in the Arctic Region In Summer) campaign database at the Earth Science Division Project Office/NASA Ames Research Center. A summary of ozonesonde stations used in this analysis is shown in Table 4. Electrochemical concentration cell (ECC) ozonesondes [*Komhyr*, 1969] were used as ozone sensors for all stations, except for Syowa where RS II-KC79D (KC) ozonesondes with carbon and platinum electrodes were used [*WMO*, 1998]. The estimated precision and accuracy in the ECC ozonesonde measurement are  $\pm 3\%$  and  $\pm 5\%$  in the stratosphere up to 10 hPa [*Komhyr et al.*, 1995]. For altitudes between 12 and 28 km, it is reported that the systematic difference between different sonde types (including ECC and KC) is within 5%, and the random variability is also smaller than 5%, when the profiles are normalized to ground-based total ozone measurements [*WMO*, 1998]. Only for the KC sondes, we used the ozone values normalized to the colocated Dobson measurements in this study. The average and 1 sigma standard deviation of the correction factors are  $0.96 \pm 0.06$ .

### 2.4. Balloon-Borne, Airborne, and Ground-Based Instruments

[14] Data from balloon, aircraft, and ground-based instruments are also used for the validation. These data have been also registered in the ILAS-CMDB, or the Network for the Detection of Stratospheric Change (NDSC) database. Observation date and time, launch (or observation) site, location (latitude and longitude), vertical resolution, and accuracy at the TH of 20 km (if such information is available), and principal investigators of each instrument are listed in Table 5. Here we describe briefly the instrumentation of each sensor.

#### 2.4.1. Balloon-Borne Instruments

[15] The Limb Profile Monitor of the Atmosphere (LPMA) is a solar occultation Fourier transform infrared (FTIR) spectrometer [*Camy-Peyret et al.*, 1993]. The micro-window used in this ozone retrieval is 3040.034–3040.848  $\text{cm}^{-1}$ . The integrated gondola was launched from Esrange (Swedish Space Corporation sounding rocket launching range), near Kiruna, Sweden (68°N, 21°E). The measurements were made during the balloon ascent and at float (occultation at local sunset).

[16] The Système d’Analyse par Observation Zénitale (SAOZ)-BAL is a balloon-borne UV-visible spectrometer

**Table 3.** A Summary of Error Analysis for the Version 5.20 Ozone Data, Part 2<sup>a</sup>

Altitude, km	Systematic Bias (ppmv)							
	AEC = 0.0005, $\text{km}^{-1}$		AEC = 0.001, $\text{km}^{-1}$					
	S(75) <sup>b</sup>	S(50) <sup>b</sup>	NAT	ICE	STS(5, 37) <sup>c</sup>	STS(33, 15) <sup>c</sup>	STS(47, 3) <sup>c</sup>	STS(60, 0.5) <sup>c</sup>
15	-0.01	0.03	-0.07	0.41	<0.01	0.07	0.08	0.07
20	-0.03	0.07	-0.16	0.90	<0.01	0.16	0.17	0.14
25	-0.06	0.15	-0.35	1.99	<0.01	0.35	0.38	0.32

<sup>a</sup>Systematic biases caused by the nongaseous component correction are listed for three selected altitudes. The error values at two selected aerosol extinction coefficients (AEC) at 780 nm are shown.<sup>b</sup>S(75) and S(50) denote 75 and 50 wt %  $\text{H}_2\text{SO}_4/\text{H}_2\text{O}$  binary solutions, respectively.<sup>c</sup>STS(5, 37), STS(33, 15), STS(47, 3), and STS(60, 0.5) denote 5, 33, 47, and 60 wt %  $\text{H}_2\text{SO}_4/37$ , 15, 3, and 0.5 wt %  $\text{HNO}_3/\text{H}_2\text{O}$  ternary solutions, respectively.

**Table 4.** A Summary of Ozonesonde and DIAL Measurements

Station	Latitude, deg	Longitude, deg	Number of Pairs	Principal Investigator	Type
<i>ILAS CMDB (124 Sondes, 11 Lidar)</i>					
Andoya	69.3	16.1	1	T. Deshler	sonde
Fairbanks	64.9	-147.9	9	K. Shibasaki	sonde
Kiruna	67.9	21.1	3	T. Deshler	sonde
Kiruna	67.9	21.1	37	H. Kanzawa	sonde
Kiruna	67.9	21.1	2	Y. Kondo	sonde
Yakutsk	62.0	129.6	9	V. Yushkov	sonde
Neumayer	-70.4	-8.2	34	H. Gernandt	sonde
Syowa	-69.0	39.6	26	H. Kanzawa	sonde
Dumont d'Urville	-66.4	140.0	3	F. Goutail and S. Godin	sonde
Dumont d'Urville	-66.4	140.0	11	S. Godin	DIAL
<i>OSDOC Database (97 Sondes)</i>					
Andoya	69.3	16.1	13	B. Bojkov	sonde
Gardermoen	60.1	11.0	3	B. Bojkov	sonde
Jokioinen	60.8	23.5	1	E. Kyro	sonde
Keflavik	64.0	-22.6	4	M. Gil	sonde
Legionowo	52.4	21.0	1	Z. Litynska	sonde
Lerwick	60.1	-1.2	4	M. Molyneux	sonde
Orland	63.4	9.2	1	B. Bojkov	sonde
Scoresbysund	70.5	-22.0	13	I. S. Mikkelsen	sonde
Sodankyla	67.2	26.4	52	E. Kyro	sonde
Sondrestrom	67.0	-50.6	5	I. S. Mikkelsen	sonde
<i>POLARIS Database (10 Sondes)</i>					
Fairbanks	64.9	-147.9	10	B. Johnson, H. Vömel, and S. Oltmans	sonde
<i>NDSC Database (21 Lidar)</i>					
Andoya	69.3	16.0	21	G. Hansen	DIAL

[Pommereau and Piquard, 1994], which makes use of the solar occultation technique from the balloon. The measurements were made during the balloon ascent and at float (occultation at local sunset).

[17] The in situ UV absorption photometer [Proffitt and McLaughlin, 1983] was operated together with the SLS and FIRS-2 instruments (described below). The data was obtained during the balloon ascent. The reported ozone

**Table 5.** A Summary of Correlative Balloon, Aircraft, and Ground-Based Measurements<sup>a</sup>

Date	Time, UT	Launch Site	Latitude, deg	Longitude, deg	Distance, km	$\delta$ UT, <sup>b</sup> hour	PI	Instrument	Accuracy, %	Vertical Resolution, km	Reference
970129	1241	Andoya	68.7	18.6	206	1.0	J.-P. Pommereau and F. Goutail	SAOZ	3-12	1	Pommereau and Piquard [1994]
970228	1441	Kiruna	68.0	23.0	180	0.5					
970228	1536		67.3	20.4	295	0.4					
970316	0435	Andoya	68.7	27.7	493	11.8					
970318	1541	Kiruna	67.4	21.1	373	1.5					
970318	1653		66.8	17.4	319	0.3					
970204	1442	Kiruna	67.7	10.6	227	0.4	H. Schlager	UV-photometer	5	-	Schlager et al. [1997]
970214	1329	Kiruna	67.6	22.1	801	0.4	K. Pfeilsticker	DOAS	1	0.3	Ferlemann et al. [2000]
970226	1350	Kiruna	67.9	22.4	490	0.6	C. Camy-Peyret	LPMA	7	2.5	Camy-Peyret et al. [1993]
970226a	1042	Kiruna	68.2	15.0	295	5.4	H. Kuellmann	ASUR	12	5-10	de Valk et al. [1997]
970226b	1056		66.7	13.5	368	5.2					
970226	2158	Kiruna	67.1	21.3	583	5.9	J.-B. Renard	AMON	5	1	Renard et al. [1996]
					577 <sup>c</sup>	7.5 <sup>c</sup>					
970425	2325	Fairbanks	65.1	-147.5	279	6.8	H. Fukunishi	TDLHS <sup>d</sup>	15	5	Fukunishi et al. [1990]
970507	2047		65.1	-147.5	428	9.0					
970508	1644		65.1	-147.5	428	10.9					
970430	1518	Fairbanks	64.8	-147.6	155	9.2	J. J. Margitan	UV-photometer	5	5 m <sup>e</sup>	Proffitt and McLaughlin [1983]
970430a	1940	Fairbanks	69.0	-149.0	698	10.0	B. Stachnik	SLS	14-21	2-3	Stachnik et al. [1992]
970430b	2150		67.8	-162.0	543	9.5					
970430a	1913	Fairbanks	68.4	-148.9	640	10.4	W. A. Traub	FIRS-2	5	4	Johnson et al. [1995]
970430b	2146		67.6	-156.2	684	9.5					
970508	1211	Fairbanks	68.6	-146.3	740	6.4	G. C. Toon	MkIV	6	2	Toon [1991]

<sup>a</sup>Measurement location, time, accuracy, and vertical resolution for a TH of 20 km are described, if such parameters are available.

<sup>b</sup>Absolute time difference between ILAS and other sensor.

<sup>c</sup>There were two coincident pairs for one AMON measurement.

<sup>d</sup>Ground-based instrument.

<sup>e</sup>Vertical resolution for 1 second data.

accuracy is 5% with 1 s time resolution which corresponds to a vertical resolution of 5 m.

[18] The Differential Optical Absorption Spectroscopy (DOAS) instrument is a UV-visible spectrometer [Ferlemann *et al.*, 2000]. The measurements were made during the balloon ascent and at float (occultation at local sunset).

[19] The Absorption par Minoritaires Ozone et NO<sub>x</sub> (AMON) is a stellar occultation UV-visible spectrometer [Renard *et al.*, 1996]. The measurements were made during the float period of the balloon flight.

[20] The Submillimeter-wave Limb Sounder (SLS) is a high resolution heterodyne radiometer-spectrometer that measures atmospheric limb thermal emission spectra of ozone at 637 GHz [Stachnik *et al.*, 1992]. Ten limb soundings were made when the balloon was at float altitude. The first three soundings were made at the gondola heading (with respect to true north) of about 3° and the latter seven soundings were made at the gondola heading of about -67°. Therefore, the locations of TH for each measurement were different from each other. The locations at the TH of 20 km for the first three soundings and the latter seven soundings were 69°N-149°W and 68°N-162°W, respectively. The estimated error for ozone is 4 to 10% for altitudes of 25 to 40 km, and around 20% at 45 km.

[21] The MkIV is a solar occultation FTIR spectrometer [Toon, 1991] that measures the entire 650-5650 cm<sup>-1</sup> spectral region simultaneously at 0.01 cm<sup>-1</sup> resolution. The ozone profile used for this study was measured from float (38 km altitude) during sunrise and is shown by Toon *et al.* [1999, Figure 4]. The reported ozone was the average of 40 different spectral intervals between 766 and 4038 cm<sup>-1</sup>, including the ν<sub>3</sub> band used by ILAS.

[22] The Far-Infrared Spectrometer (FIRS)-2 is a FTIR spectrometer that measures atmospheric thermal emission in the wave number range of 75-1300 cm<sup>-1</sup> [Johnson *et al.*, 1995]. Ozone is retrieved from the average of retrievals from two spectral regions: 80-130 cm<sup>-1</sup> and 760-820 cm<sup>-1</sup>. The ozone profile used in this study is shown by Jucks *et al.* [1998, Figure 1a]. Two limb soundings were made when the balloon was at float altitude. The locations at the TH of 30 km for the first and second soundings were 68.4°N-148.9°W and 67.6°N-156.2°W, respectively.

#### 2.4.2. Airborne Instruments

[23] The Airborne Submillimeter SIS Radiometer (ASUR) is a passive submillimeter-wave heterodyne receiver measuring thermal emission lines of stratospheric trace gases in the 624 to 654 GHz spectral region [de Valk *et al.*, 1997]. The instrument was operated on board the German research aircraft "Falcon" based at Kiruna airport. The vertical resolution of the retrieved ozone profiles is 5-10 km in the lower stratosphere and 10-20 km in the upper stratosphere. The reported error for ozone is 12, 14, and 12% for altitudes of 20, 30, and 40 km, respectively.

[24] The in situ UV absorption photometer [Schlager *et al.*, 1997] was operated on board the Falcon aircraft. The reported data were integrated over 60 s and the accuracy was of the order of 5% for the ozone data.

#### 2.4.3. Ground-Based Instruments

[25] The Tunable Diode Laser Heterodyne Spectrometer (TDLHS) is a high spectral resolution infrared spectrometer

[Fukunishi *et al.*, 1990]. The solar absorption spectra at around 1133 cm<sup>-1</sup> with a resolution of 0.0013 cm<sup>-1</sup> were observed at Poker Flat near Fairbanks. The reported accuracy used in this study was 15% for 5 km vertical resolution.

[26] The Differential Absorption Lidar (DIAL) was operated at the Antarctic station Dumont d'Urville (67°S, 140°E) [Godin *et al.*, 2001]. It uses the two wavelengths of 308 nm (absorbed) and 353 nm (reference). The vertical resolution is 1.4 km at 20 km altitude and 3.0 km at 30 km altitude. The reported errors used in this study were 3 and 10% at 20 and 30 km altitudes, respectively. The number of data used here is shown in Table 4. These coincidence measurement pairs were found from May and June 1997.

[27] Data from the DIAL at the Arctic Lidar Observatory for Middle Atmosphere Research (ALOMAR) station, Andoya, Norway (69°N, 16°E) [Hansen and Chipperfield, 1999] are also used for this validation study. These data are archived in the NDSC database. The reported error used in this study was 4, 2, and 5% at 20, 30, and 40 km altitudes, respectively. The number of data used here is shown in Table 4. These coincidence measurement pairs were found from November 1996 and January-April 1997.

### 3. Criteria for Comparisons

#### 3.1. Data Selection

[28] Recently, the "Lagrangian approach" is used for searching for coincidence measurement pairs [Lu *et al.*, 2000; Morris *et al.*, 2000]. Morris *et al.* [2000] suggested that results obtained using this approach are equivalent to or improve upon results obtained using a "traditional approach." Although this approach is very powerful in order to increase the number of pairs without degradation of the comparison result, we do not use it in this study since we could find enough events using the traditional approach and we performed comparisons up to 70 km where we have no wind data for the Lagrangian approach. For making validation studies, criteria with regard to latitude and longitude differences with more relaxed longitude criteria are generally used. However, we did not use the relaxed longitude criteria for the following reasons. For comparisons in the high latitudes, data were taken inside, at the boundary, and outside of polar vortices in winter-spring time. Therefore, there are large inhomogeneities in the ozone distribution. Although the stratosphere in the summer time is less dynamically disturbed, the ozone data at the high latitudes also show some inhomogeneity even in the summer time [Brühl *et al.*, 1998; Hoppel *et al.*, 1999; Park and Russell, 1994]. Here, we used criteria in universal time (UTC) and space differences to be ±12 hours and 300 km, respectively, in order to extract the coincidence pairs between ILAS and other satellite sensors of SAGE II, HALOE, and POAM II. For searching coincidence measurements, location and time at TH of 20 km were used as the representative location and time of each measurement.

[29] Both ILAS and POAM II were carried on polar orbiting satellites, each having almost the same orbital elements, so each occultation event was occurring continuously at high latitudes and coincidentally in time and

**Table 6.** A Summary of Coincident Measurements for Each Period From November 1996 to June 1997

Period	Number <sup>a</sup>	Distance, <sup>b</sup> km	Time, <sup>c</sup> hour	Hemisphere <sup>d</sup>	Occultation Mode <sup>e</sup>	
					ILAS	Validation
HALOE–ILAS (total number = 202)						
19–24 November	40	172 (28)	1.8 (3.5, 0.0)	SH	SS	SR
10–16 December	39	204 (130)	1.6 (3.5, 0.0)	SH	SS	SS
28–31 January	17	178 (19)	4.5 (5.3, 3.8)	SH	SS	SR
18–20 February	22	165 (64)	0.5 (1.0, 0.1)	SH	SS	SS
24 March to 2 April	59	166 (23)	0.2 (0.5, 0.0)	NH	SR	SS
13–14 May	12	147 (9)	6.9 (7.4, 6.5)	NH	SR	SR
16–18 June	13	248 (197)	0.2 (0.4, 0.0)	NH	SR	SS
SAGE II–ILAS (total number = 149)						
4–24 November	74	149 (45)	1.4 (3.2, 0.0)	SH	SS	SR, SS
8–30 January	34	213 (136)	4.0 (4.8, 3.1)	SH	SS	SR, SS
3–4 February	20	194 (125)	0.5 (1.2, 0.0)	SH	SS	SS
26–29 April	10	188 (125)	7.9 (8.3, 7.4)	NH	SR	SR
28–30 May	11	220 (157)	0.2 (0.4, 0.0)	NH	SR	SS
POAM–ILAS (total number = 120)						
1–13 November	67	155 (77)	0.6 (1.0, 0.0)	SH	SS	SS
6–13 November	53	170 (86)	0.2 (0.5, 0.0)	NH	SR	SR

<sup>a</sup>Numbers of coincident measurement profiles for each period.

<sup>b</sup>Average of individual distance between observed locations with a criterion of 300 km separation. Minimum distance is shown in the parentheses.

<sup>c</sup>Average of individual time difference between observation times with a criterion of  $\pm 12$  hours. Maximum and minimum time differences are shown in the parentheses, respectively.

<sup>d</sup>SH and NH are for solar occultations occurring in the SH and the NH, respectively.

<sup>e</sup>SS and SR are for solar occultations occurring at sunset and sunrise as seen from the satellites, respectively.

location, as shown in Figure 1. Unfortunately, POAM II measurement ceased on 14 November 1996, thus no correlative data were available thereafter. Since SAGE II and HALOE are carried on inclined-orbit satellites, the occultation events occur globally. Therefore, coincidence measurements of SAGE II and HALOE with ILAS were limited in time and space as shown in Figure 1. With the criteria defined above, 149 coincidence pairs for SAGE II and ILAS (hereafter referred to as SAGE II–ILAS), 202 pairs for HALOE–ILAS, and 120 pairs for POAM II–ILAS were selected in a first step. A summary of the coincidence measurements of satellite sensors is listed in Table 6, separately for the periods shown in the table. The maximum time difference was 8.3 hours, which was found from the SAGE II–ILAS pairs.

[30] For correlative ozonesonde measurements with ILAS, we used criteria in time and space to be  $\pm 12$  hours and 500 km. The criterion in space was extended to 500 km in order to increase the number of coincidence measurements. As the representative location and time of the ozonesonde measurements, those at the measurement point of 20 km altitude were used if such information was available (otherwise the location of each launch site was used). In total, 206 coincidence pairs between ILAS and ozonesondes were selected from 13 stations in the NH and 3 stations in the SH in a first step. A summary of the coincidence measurements of ozonesondes is listed in Table 4.

[31] For measurements by balloon, aircraft, and ground-based instruments, we also used criteria in time and space to be  $\pm 12$  hours and 500 km. Nevertheless, we relaxed the criterion in space to be 1000 km for extracting data obtained by DOAS, AMON, SLS, MkIV, and FIRS-2, which do not fulfill the 500 km criterion, as listed in Table 5. As the representative location and time of these measurements, those at the measurement (or tangent) point

of 20 km altitude were used if such information was available (otherwise the locations at each launch site were used).

### 3.2. Consistency of Altitude to be Compared

[32] In order to compare profiles between ILAS and validation data, the vertical grid (or resolution) should be consistent with each other. As listed in Table 1, THs from satellite sensors are registered as geometric altitude with different spacing. For the HALOE data, we first linearly interpolated ozone partial pressures and atmospheric pressures to 0.1 km altitude grid. Then these data were averaged within each 1 km altitude bin centered at each  $i$  km grid ( $i$ : integer), resulting in ozone mixing ratios. For the SAGE II data, ozone mixing ratios were averaged every 3 points centered at  $i$  km. Altitudes for ozonesondes are registered at about 100 m intervals with geopotential altitude, which are then converted to geometric altitudes. Then, the ozone partial pressures and atmospheric pressures were integrated within each 1 km bin centered at each  $i$  km grid, resulting in ozone mixing ratios. For balloon, aircraft, and ground-based instruments, the methods used to match the altitude grid and/or vertical resolution are explained in section 4.3. For this comparative study, we used data obtained between 9 and 70 km for comparisons with satellite, balloon, aircraft, and ground-based sensors and between 9 and 30 km for those with ozonesondes, within the available data range.

### 3.3. Data Filtering

[33] In the NH, the polar vortex formed in December 1996 and remained exceptionally late; until early in May 1997 in the lower stratosphere, as seen from *Northern Hemisphere Winter Summary 1999–2000* [NOAA, 2000a, Figure 8]. In the spring of 1996 in the SH, the polar vortex existed until the beginning of December 1996 in the lower

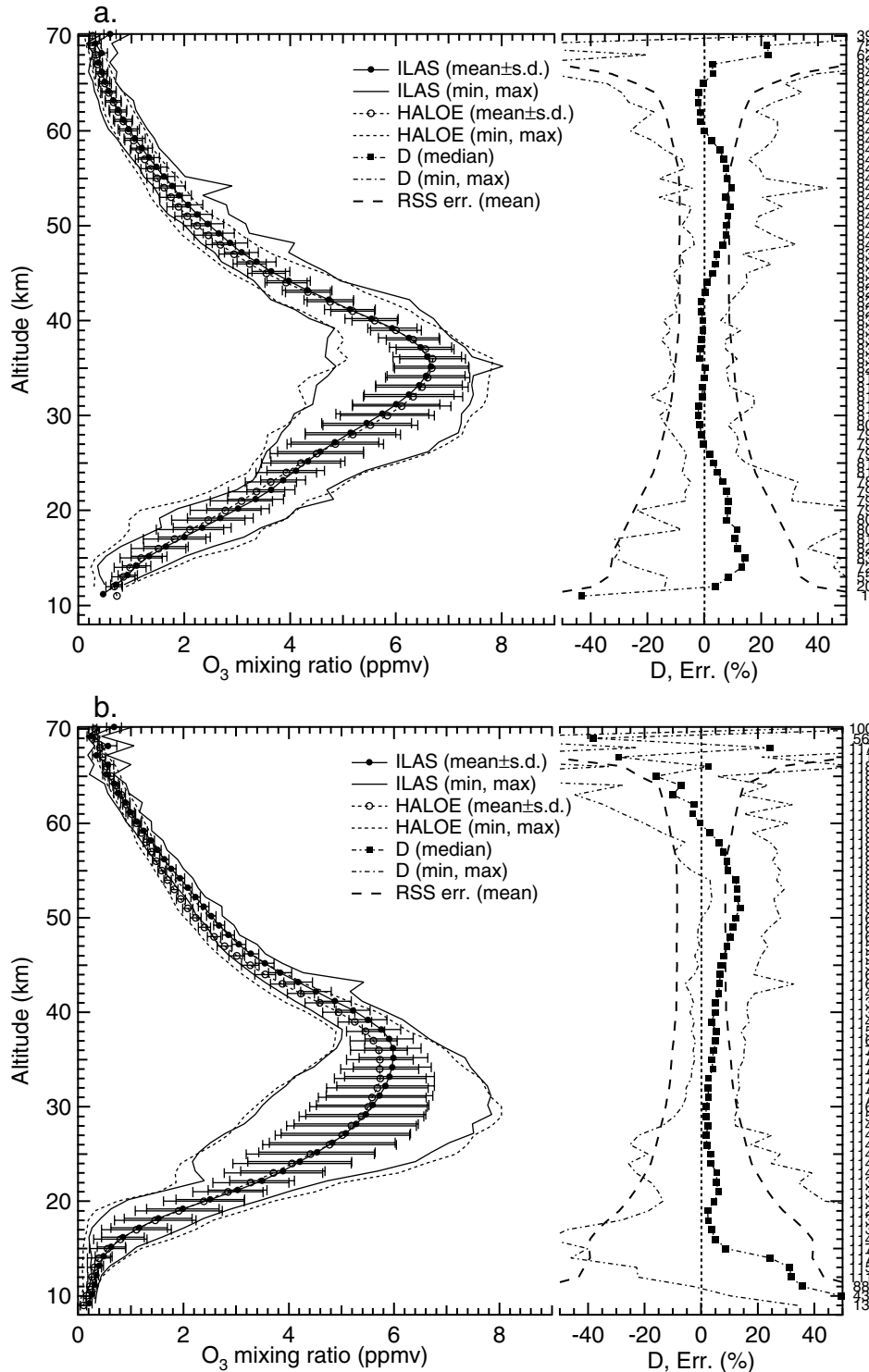


**Figure 2.** (a) Average profiles of ozone mixing ratios retrieved by ILAS and HALOE in the NH (left panel). The ILAS data are plotted with 0.2 km shift for clarity. Numbers of coincidence measurement pairs at each altitude are shown on the right-hand side of the figure. Error bars show one sigma standard deviation of the data at each altitude. Maximum and minimum values of the data are shown as a solid line (ILAS) and a dotted line (HALOE), respectively. The median profile of individual percentage differences, labeled as D (see text for the definition), between ILAS and HALOE ozone mixing ratios is also shown (right panel). Maximum and minimum values of the data are shown as dash-dotted lines. Dashed lines symmetrical with respect to the zero line show the average of individual RSS total uncertainties, labeled as RSS err., in ILAS and HALOE measurements (see text). (b) Same as Figure 2a, but in the SH.

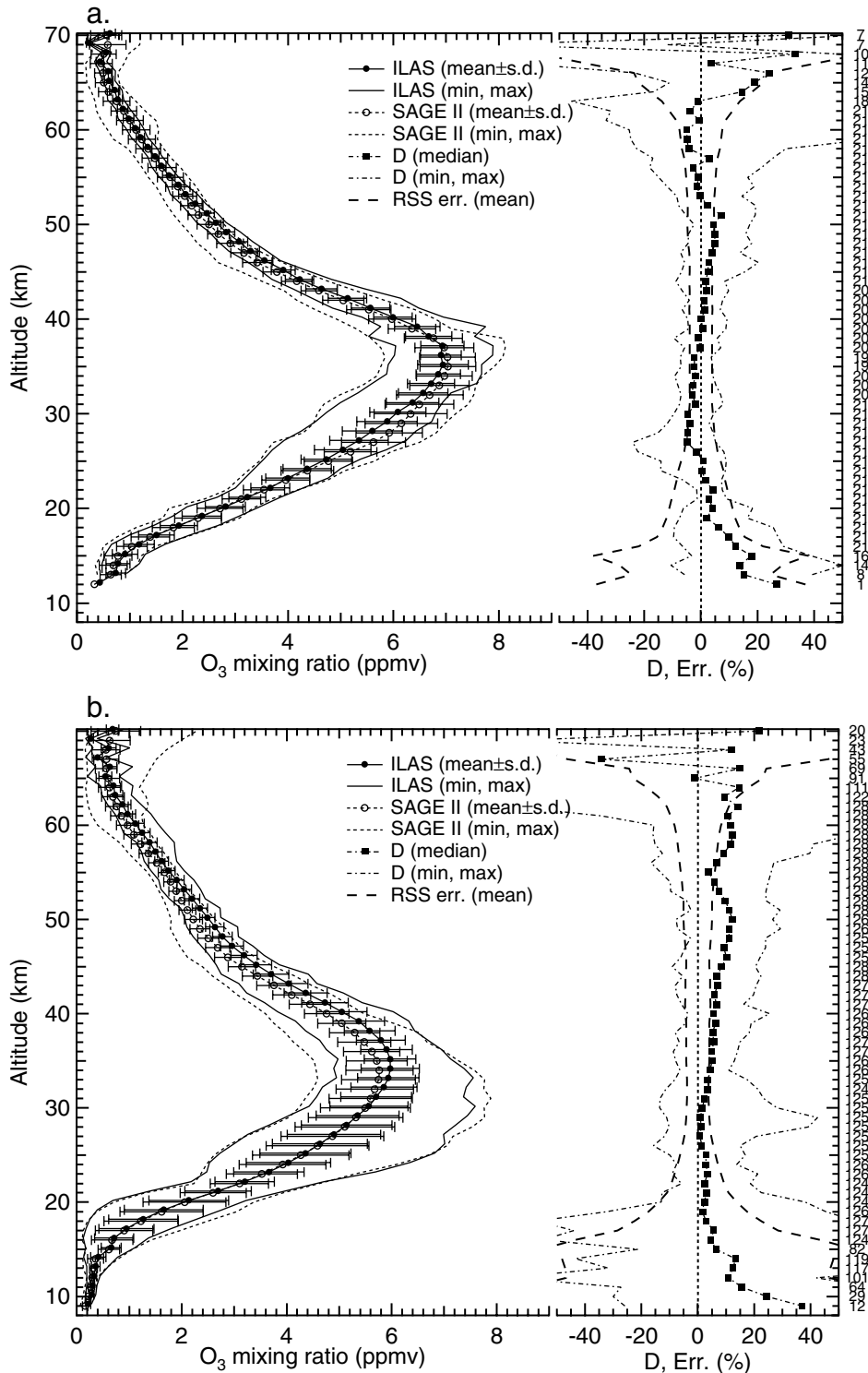


**Figure 3.** (a) Same as Figure 2a, but for ILAS and SAGE II in the NH. (b) Same as Figure 2a, but for ILAS and SAGE II in the SH.

stratosphere, as seen, for example, from *Southern Hemisphere Winter Summary 2000* [NOAA, 2000b, Figure 12]. As suggested by Lu et al. [2000], for comparative studies, potential vorticity (PV) analysis should be incorporated to find better coincidence pairs in terms of meteorological conditions during the winter periods.

[34] With this in mind, the coincidence pairs selected by the above criteria were further screened by the following procedure. First, PV values at each TH location and time for ILAS and its coincidence measurements were calculated using the United Kingdom Meteorological Office (UKMO) assimilation data [Swinbank and O'Neill, 1994], which were

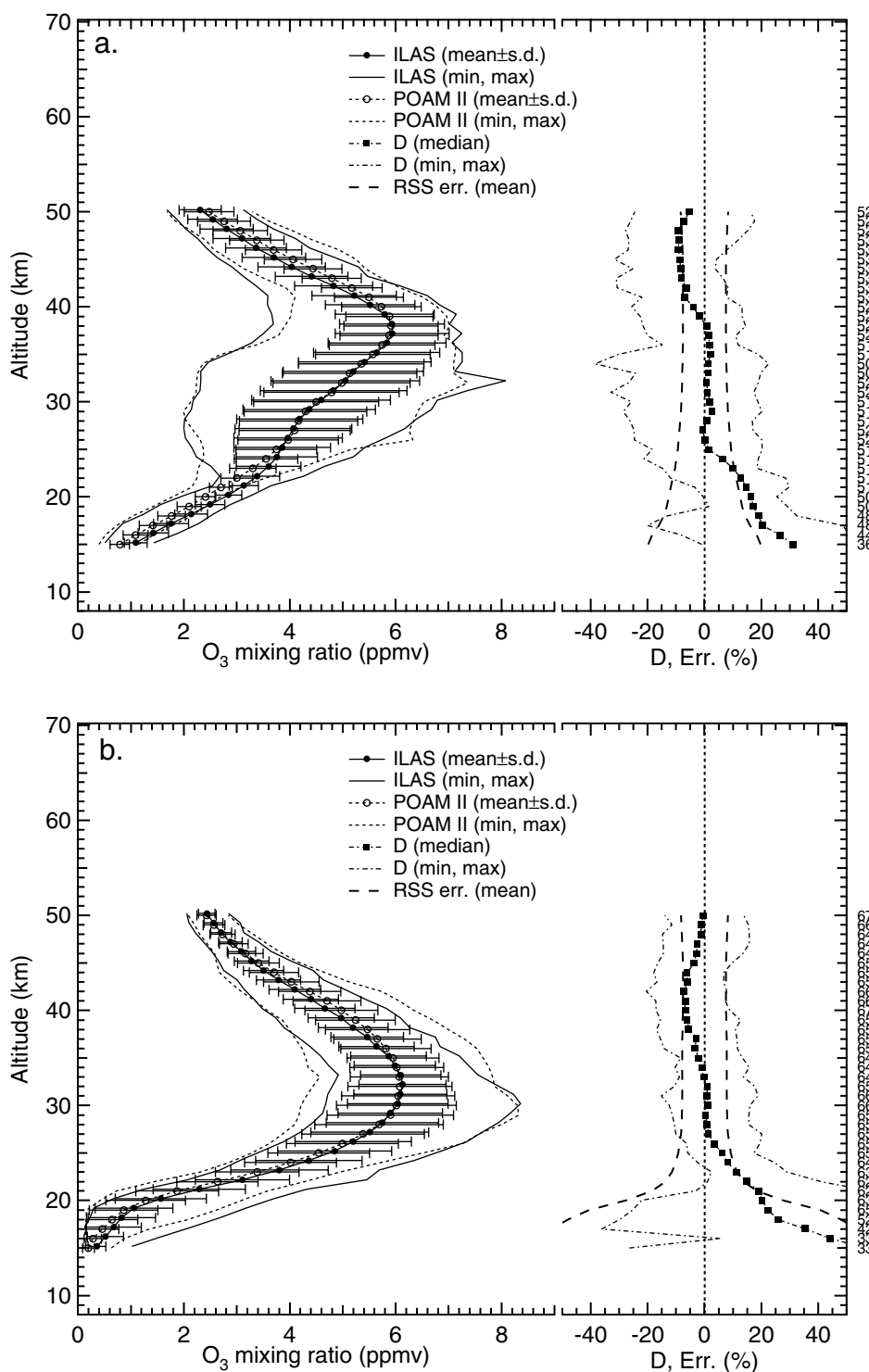


**Figure 4.** (a) Same as Figure 2a, but for ILAS and POAM II in the NH. (b) Same as Figure 2a, but for ILAS and POAM II in the SH.

supplied as 24-hourly data at 12 UTC. The horizontal resolution of the data is  $2.5^\circ$  in latitude and  $3.75^\circ$  in longitude. The vertical resolution of the data corresponds to the UARS standard pressure grid ( $P_i$  (hPa) =  $1000.0 \times 10^{(-i/6)}$ ,  $i = 0, 1, \dots, 21$ ). PV values and potential temperatures were calculated at each grid point. These data were then

interpolated in time and space to each measurement (both for ILAS and its correlative measurement) with 1 km geometric altitude grid. We calculated relative differences defined as  $2 * \{PV(ILAS) - PV(val)\} / \{PV(ILAS) + PV(val)\}$  for each 1 km altitude grid where PV(ILAS) and PV(val) denote PV values at the time and location of ILAS and validation

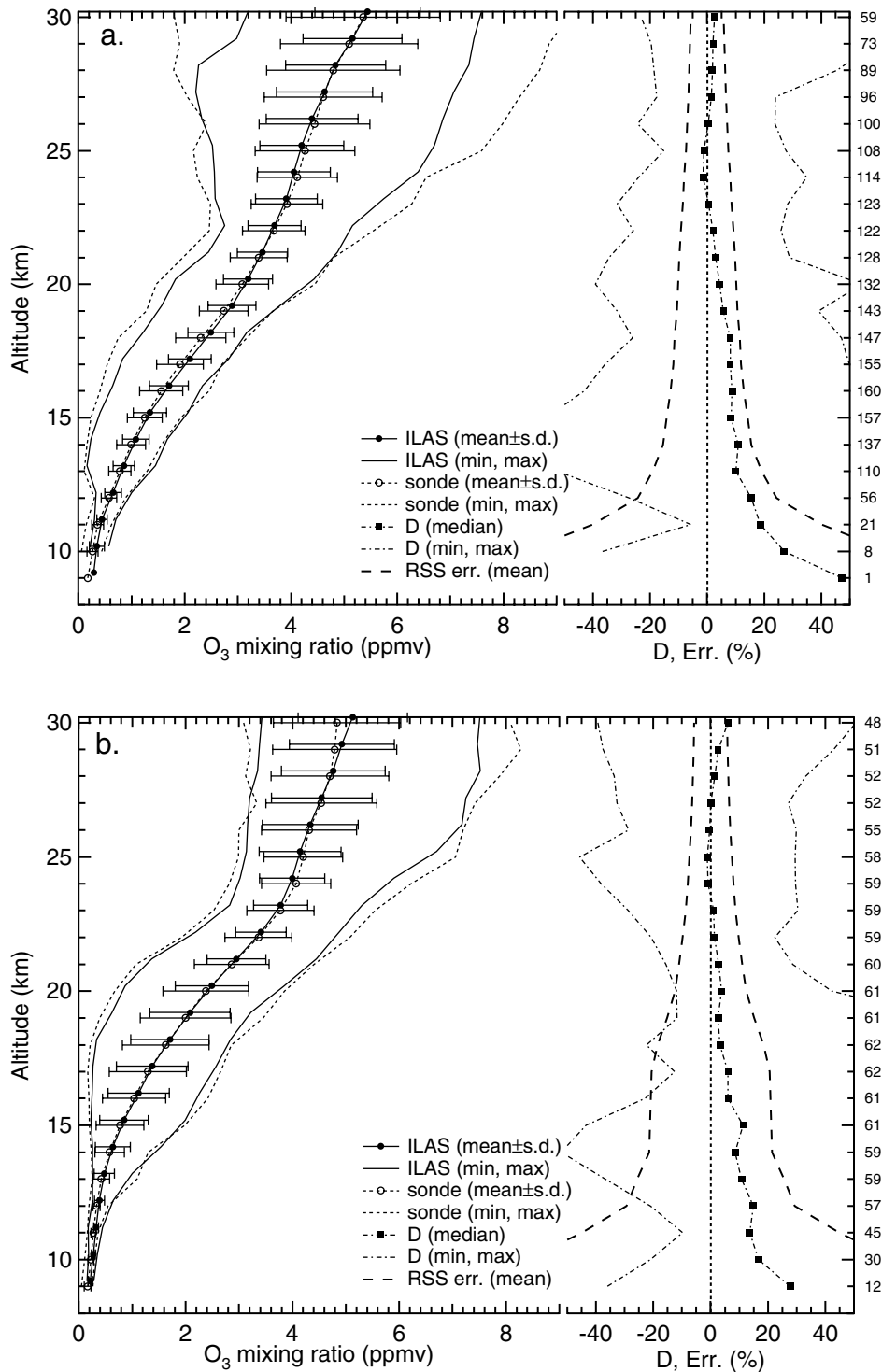


**Figure 5.** (a) Same as Figure 2a, but for ILAS and ozonesondes in the NH. (b) Same as Figure 2a, but for ILAS and ozonesondes in the SH.

measurements. If the difference exceeds  $\pm 15\%$  at consecutive altitudes for more than 3 km, the data at these altitudes were discarded from this validation analysis. Although we made comparisons between ILAS and several sensors providing 5 km or 11 km column (see section 4.3), there was no PV difference exceeding 15%. Then, if the ozone value was

smaller than its measurement uncertainty (which was described in section 2), that ozone value was also filtered out. This data filtering suppresses comparisons at small ozone values (a few hundred ppbv level), with large relative errors. Finally, but only for the ozonesondes profiles, if anomalies in ozone values were seen at any altitude (such

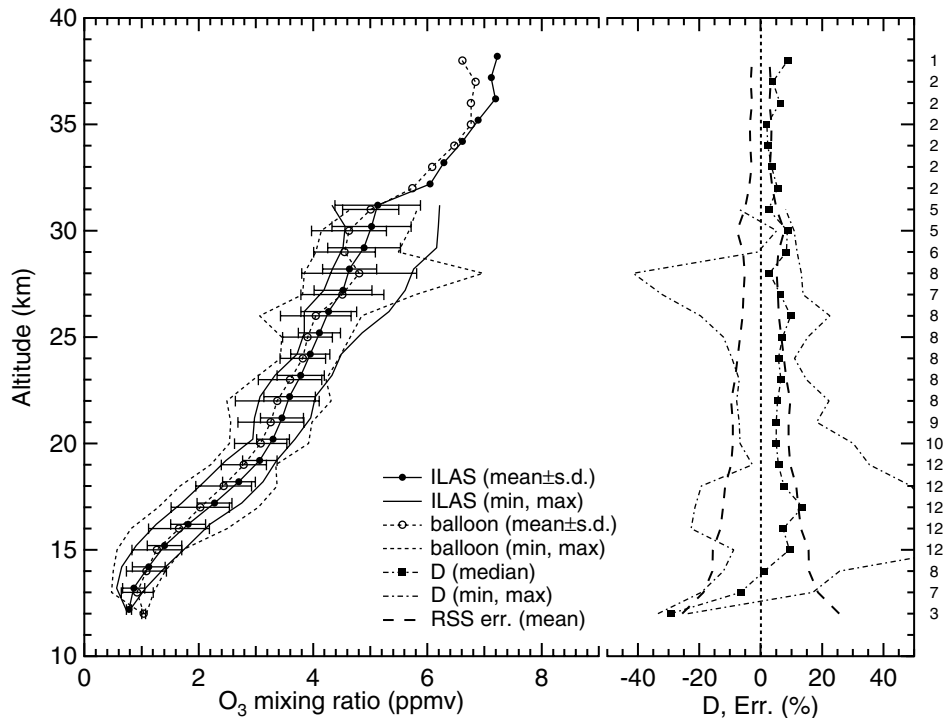


**Figure 6.** Same as Figure 2a, but for ILAS and several remote sensing and in situ instruments for the period of January–March 1997 near Kiruna, Sweden, and for the period of April and May 1997 near Fairbanks, Alaska.

as sudden negative or positive dips in ozone and/or pressure data probably due to unidentified perturbations, or anomalous decrease in ozone data at higher altitudes probably due to reduced pump performance or evaporation of sensing solutions, and so on), these altitudes were also rejected.

## 4. Comparisons

### 4.1. Satellite Sensors

#### 4.1.1. HALOE

[35] Figures 2a and 2b show average profiles of ozone measured by ILAS and HALOE between 9 and 70 km in the NH and SH, respectively, together with minimum, maximum, and 1 sigma standard deviation of the data (left panel). In the right panel, the median of individual percentage differences,  $D$ , between ILAS and HALOE is shown, together with its minimum and maximum. Here,  $D$  is a relative difference defined as:

$$D(\%) = 100 \times 2 \times \frac{\{O_3(\text{ILAS}) - O_3(\text{val})\}}{\{O_3(\text{ILAS}) + O_3(\text{val})\}} \quad (1)$$

where  $O_3(\text{ILAS})$  and  $O_3(\text{val})$  show ozone mixing ratios of ILAS and validation data (from any of the correlative sources like HALOE, SAGE II, POAM II, ozonesonde, or balloon, aircraft, and ground-based instruments) at each geometric altitude grid, respectively. The number  $N$  of coincidences or measurement pairs at each altitude is shown on the right-hand side of the figure. Two dashed lines symmetrical with respect to the zero line show averages

of RSS of the errors in the ILAS and HALOE measurements at each altitude, defined as:

$$\text{RSS error (mean)} = \sum_i^N \sqrt{\text{Err}_i(\text{ILAS})^2 + \text{Err}_i(\text{val})^2} / N \quad (2)$$

$(i = 1 \text{ to } N)$

where  $\text{Err}(\text{ILAS})$  and  $\text{Err}(\text{val})$ , respectively, show total measurement errors of ILAS and validation data, which were described in section 2. In the NH comparison (Figure 2a), the  $D$  values were within  $\pm 5\%$  between 24 and 47 km, revealing an excellent agreement. Between 12 and 23 km, the  $D$  values exceeded 5% but were within 15% at worst, and less than half of the RSS error. Between 48 and 58 km, the  $D$  values again exceeded 5% but were within about 10%, which is comparable to the RSS error in this altitude region. The absolute values of  $D$  were also smaller than 5% between 59 and 67 km. However, above 65 km, the RSS errors are quite large (up to 90% at 70 km altitude), so we do not consider that region. In general, no statistically significant bias, exceeding the RSS error, in the ILAS ozone measurements for the NH was recognized from comparisons with the HALOE measurements.

[36] For the SH comparison (Figure 2b), it can be seen that the  $D$  values increased with increasing altitude above 30 km up to around 51 km. Between 48 and 55 km, the  $D$  values exceeded the RSS error, suggesting that some high bias in the ILAS data exists for these altitudes when compared with the HALOE data. Above 56 km, the  $D$  values were generally less than the RSS error in these altitudes, although some oscillations were seen in the  $D$  values resulting from oscillations in the retrieved ILAS data.

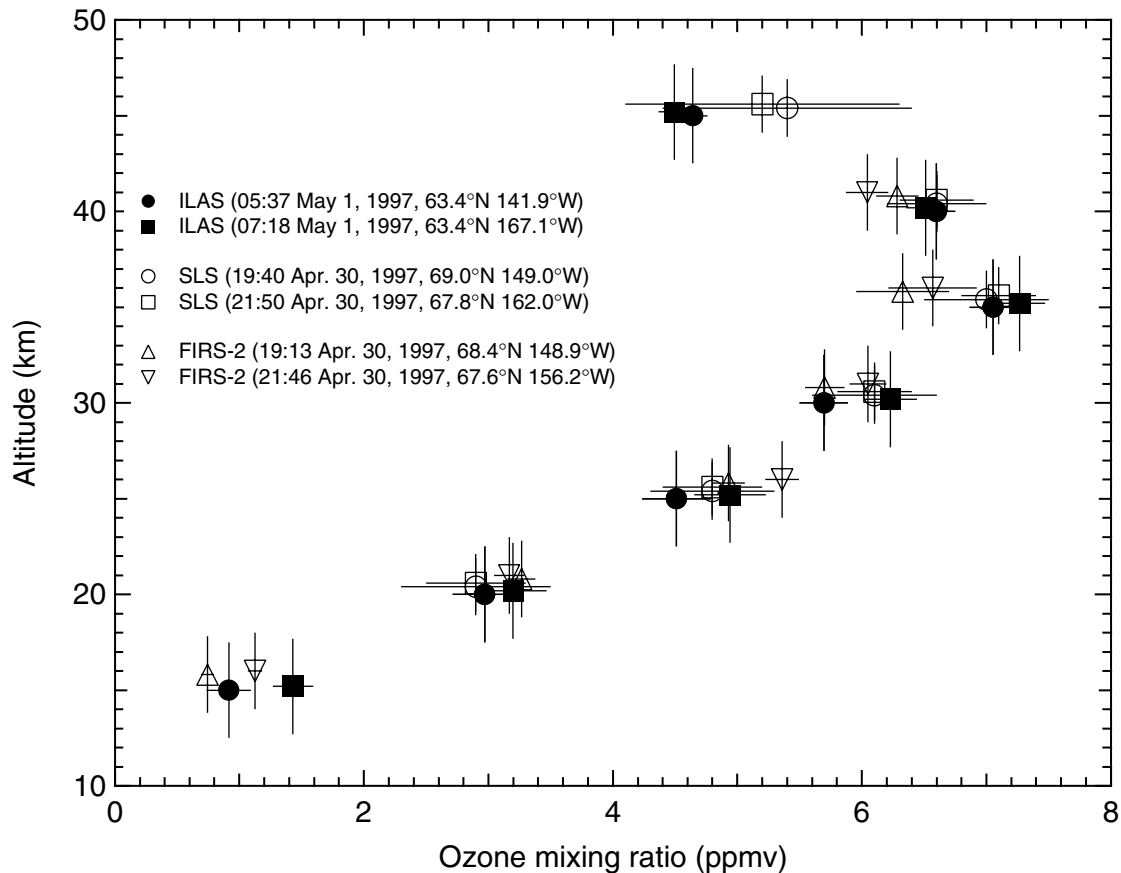


**Figure 7.** Profiles of SLS and FIRS-2 data together with coincident ILAS data. Data are plotted with 0.2 km shifts for clarity.

Between 15 and 47 km, the D values were within 5% and also less than the RSS error in these altitudes. Between 9 and 14 km, the D values increased with decreasing altitude, reaching more than 50% at the lowermost layers. It should be noted, however, that such large D values correspond to absolute differences ranging from 0.09 to 0.11 ppmv. It should also be noted that the level of these absolute differences is comparable to the level of total error of the version 5.20 ILAS ozone in this altitude range. No statistically significant bias in the SH ILAS ozone data was generally recognized, except for the altitude region of 48–55 km. We will discuss this discrepancy for this altitude range in section 5, in terms of the time difference of the measurements.

**4.1.2. SAGE II and POAM II**

[37] Similar to Figure 2, Figures 3a and 3b show average profiles of ozone measured by ILAS and SAGE II (left panel) and a profile of the D value (right panel) between 9 and 70 km in the NH and SH, respectively. As was seen from the ILAS–HALOE comparisons, similar features are evident: (1) the D values were almost within  $\pm 10\%$  for all altitudes in the NH comparison, except for altitudes below 16 km and above 64 km, (2) the D values increased with increasing altitude above 30 km up to around 50 km in the SH comparison. The D values in the SH exceeded the RSS error above about 35 km altitude. However, these D values were 12%, at worst, below 60 km. Except for the high altitude region, no statistically significant bias in the ILAS

ozone measurements for both hemispheres can be recognized from comparisons with the SAGE II measurements.

[38] Average profiles of ozone measured by ILAS and POAM II and a profile of the D value between 15 and 50 km in the NH and SH are shown in Figures 4a and 4b, respectively. For both hemispheres, the D values were within  $\pm 10\%$  and smaller than the RSS errors between 23 and 50 km, suggesting that no statistically significant bias in the ILAS ozone measurements is present in this altitude region. Below 22 km in the NH comparison, the D values increased with decreasing altitude and reached 30% at 15 km. It corresponds to a 0.31 ppmv absolute difference. Also, below 23 km in the SH comparison, the D value reached 56% at 15 km. However, it corresponds to a 0.16 ppmv absolute difference.

**4.2. Ozonesondes**

[39] For the lower stratosphere, the ozonesonde data are thought to be very reliable, because the sensor has a precision of 5% and altitude is precisely determined from in situ temperature and pressure measurements. However, these sensors have some time constants [Komhyer *et al.*, 1995], so a systematic shift of ozone concentration in the vertical could occur. Nevertheless, this type of data was used as validation data in order to determine the accuracy for the version 3.10 ILAS ozone data by Sasano *et al.* [1999a], as well as for other satellite measurements [e.g., Bhatt *et al.*, 1999; Cunnold *et al.*, 1989; Deniel *et al.*, 1997;

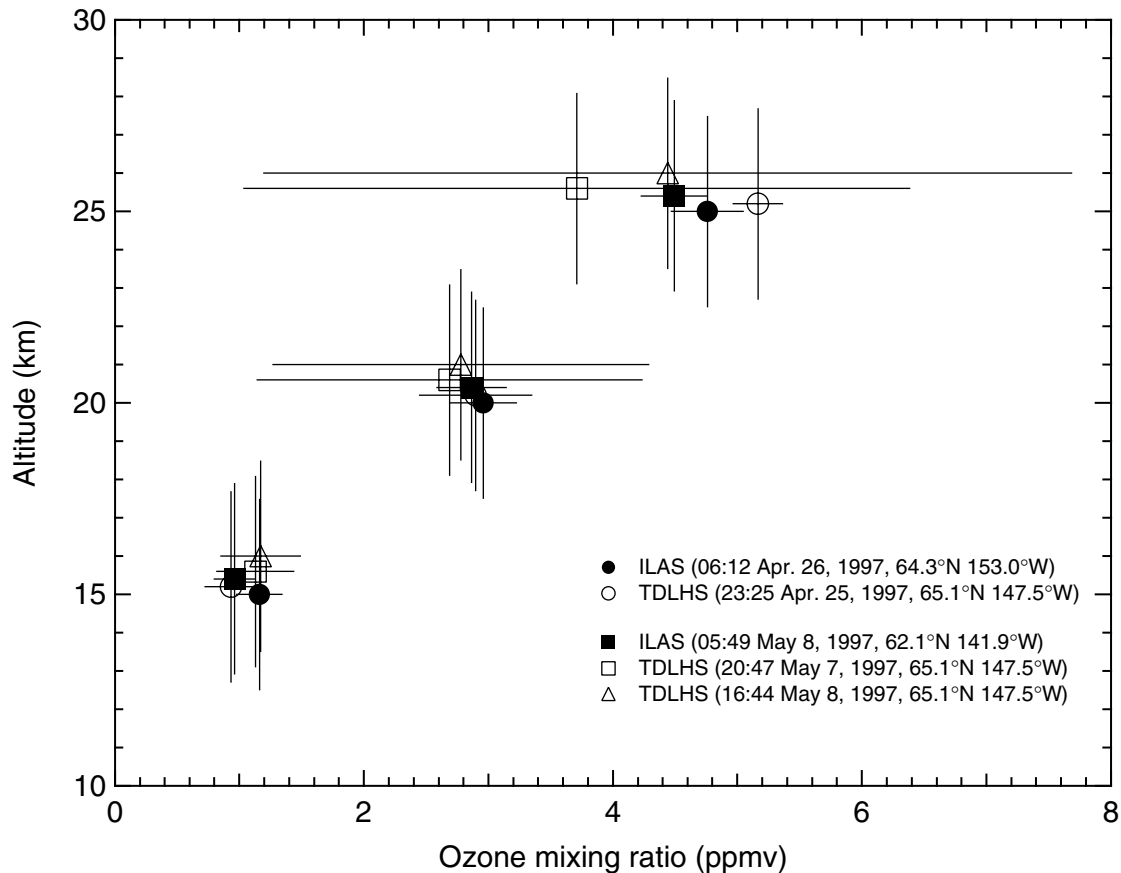


**Figure 8.** Profiles of TDLHS data together with coincident ILAS data. Data are plotted with 0.2 km shifts for clarity.

Lu *et al.*, 1997]. As for all satellite measurements, care should be taken, however, because the volume of the air mass sampled by the ozonesonde is quite different in size from the volume sampled by ILAS. Figures 5a and 5b show average profiles of ozone measured by ILAS and ozonesondes and a profile of the D value between 9 and 30 km for the NH and SH, respectively. Between 13 and 30 km, the ILAS and ozonesonde data agree quite well (within  $\pm 10\%$ ) for both hemispheres.

[40] For lower altitudes, the D values increased with decreasing altitude. This feature mimics the results from the ILAS–other satellite comparisons mentioned above. The D values reached about 27% at 9–10 km altitude for both hemispheres, but were far smaller than the RSS errors at these rather low altitudes. The difference in mixing ratio is, however, small, ranging from 0.05 to 0.11 ppmv.

### 4.3. Balloon-Borne, Airborne, and Ground-Based Instruments

[41] The altitude registration for balloon-borne sensors is well determined by a Global Positioning System (GPS) measurement. The airborne and ground-based measurements also perform a better altitude registration compared to the satellite measurements. Therefore, these correlative data sources are also suitable for validating the satellite sensor data. The ground-based instrument, TDLHS, and the instruments on board the balloon or aircraft have rather different vertical resolutions. Therefore, we sorted them into

two categories in terms of the vertical resolution. For the DIAL data, comparisons will be made at the end of this section. For instruments with a vertical resolution comparable to or better than ILAS, we just compared them on a 1 km geometric height grid. The LPMA, SAOZ, AMON, DOAS, MkIV, and JPL UV-photometer are in this category. The JPL UV-photometer data is also processed into 1 km geometric height grid in the same way as was done for the ozonesonde data (see section 3.2). In total, 12 coincident measurement pairs (see also Table 5) were selected; the averaged profile is shown in Figure 6, in the same manner as for previous figures. The ILAS data agree well with these correlative measurements, with differences roughly within  $\pm 10\%$  between 13 and 38 km. These differences are of the same magnitude as the RSS error in this altitude range.

[42] We also used data obtained by sensors with lower altitude resolution than ILAS, namely, FIRS-2, TDLHS, and ASUR because we can evaluate the degree of agreement between ILAS and the validation data for ozone partial columns even with the sensors. The balloon-borne sensor FIRS-2 has somewhat worse vertical resolution (4 km) than that of ILAS. Although the SLS instrument has a 2–3 km vertical resolution, we compare it together with the FIRS-2 instrument, because these two instruments were flown on the same gondola and measured similar air masses. In order to degrade the vertical resolution of ILAS, the ozone mixing ratio data were first converted to partial pressures by using the UKMO data. Then the data within the 5 km altitude bin

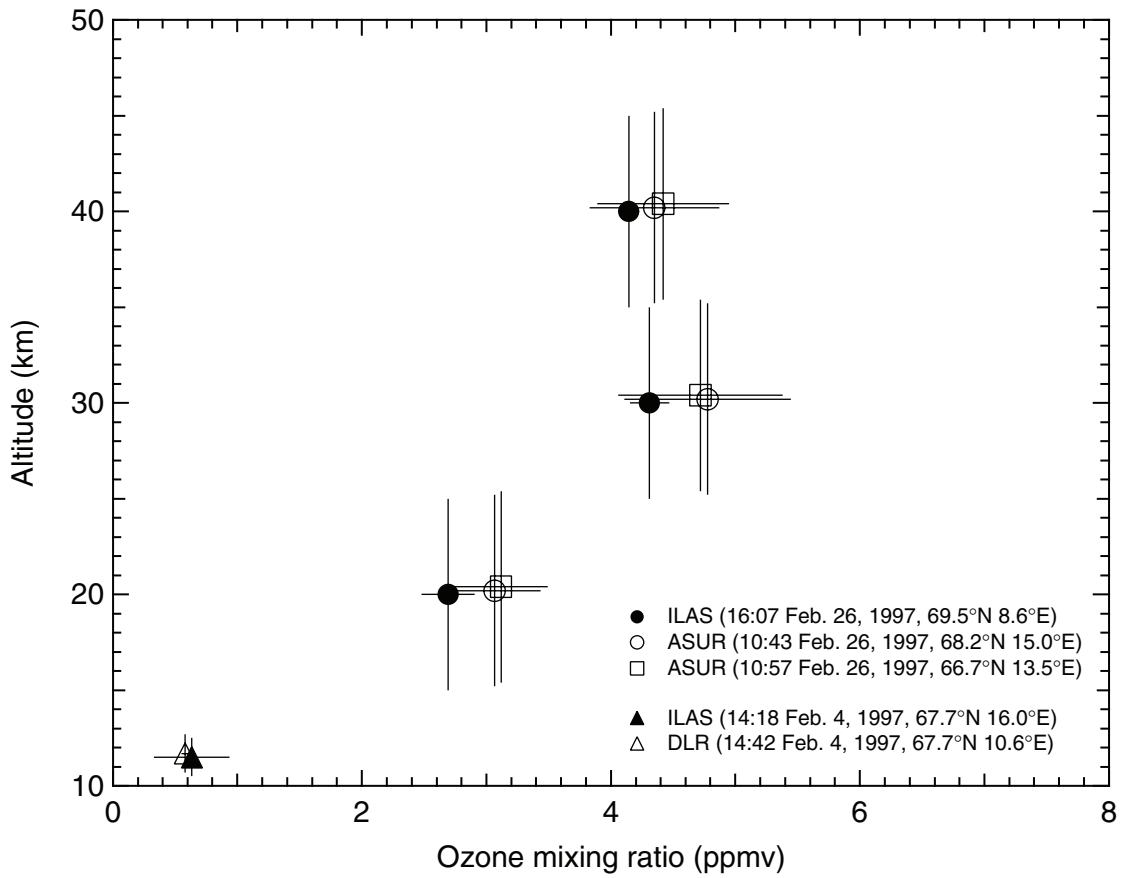


**Figure 9.** Profiles of ASUR and DLR UV-photometer data together with coincident ILAS data. Data are plotted with 0.2 km shifts for clarity.

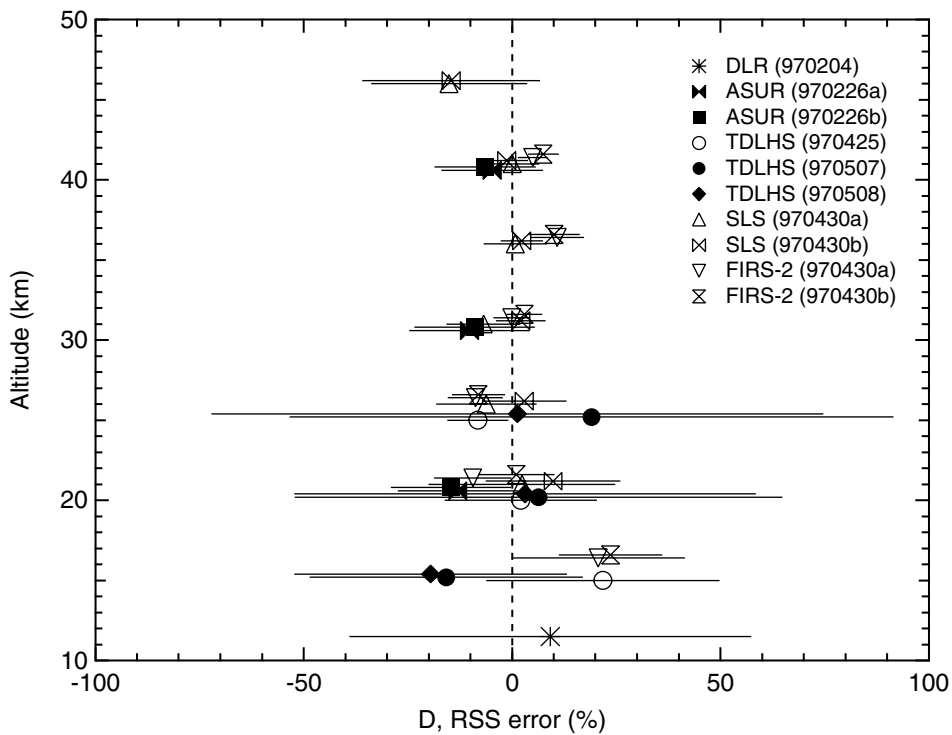


**Figure 10.** Profiles of D value for SLS, FIRS-2, TDLHS, ASUR, and DLR UV-photometer. Data are plotted with 0.2 km shifts for clarity.

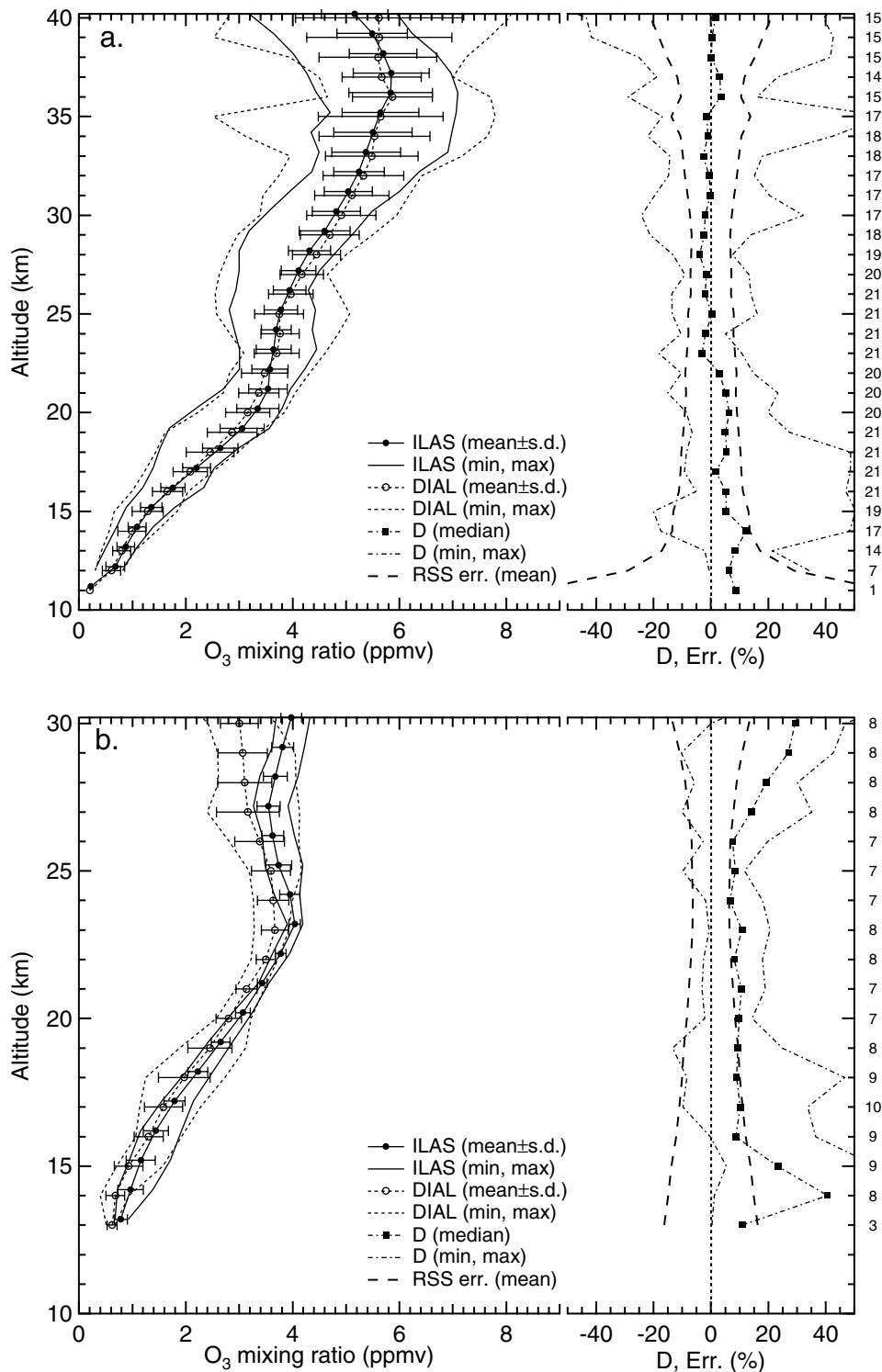


**Figure 11.** (a) Same as Figure 2a, but for ILAS and DIAL for the period of November 1996 to April 1997 at ALOMAR, Andoya, Norway. (b) Same as Figure 2a, but for ILAS and DIAL for the period of May–June 1997 at Dumont d’Urville, Antarctic.

centered at  $i \times 5$  km ( $i = 3$  to 8) are averaged, resulting in volume mixing ratio at every 5 km. These profiles together with correlative FIRS-2 and SLS profiles are shown in Figure 7. Since the vertical resolution of the SLS data at the altitude of 45 km was more than 8 km, the ILAS data

have been converted to this resolution. The ground-based sensor, TDLHS, and the two airborne sensors, ASUR and DLR UV-photometer, are shown in Figures 8 and 9, respectively, together with coincident ILAS data. Series of 6, 12, and 6 profiles were obtained by TDLHS on 25 April,

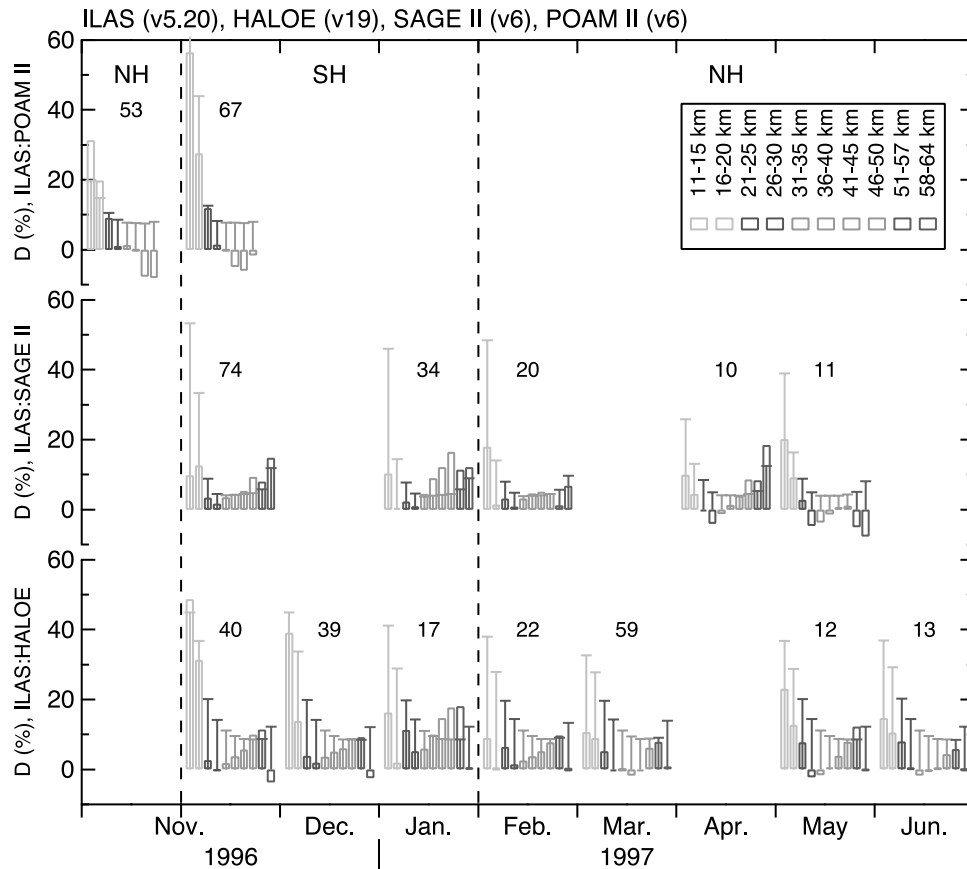


**Figure 12.** Mean relative differences between ILAS and the coincident data of satellite sensors for each 5 or 7 km layer. Numbers of coincident measurement profiles are also shown in each subpanel. See color version of this figure at back of this issue.

7 May, and 8 May, respectively. The averaged values and their one sigma standard deviations are shown for each day. These error bars were larger than the measurement error of 15% on 7 and 8 May, because spectra obtained on these days were affected by some instrumental noise. For comparisons with TDLHS and ASUR, the ILAS data were also converted to 5 km or 11 km altitude resolution in the same way as was done for the SLS and FIRS-2 data. For comparison with the DLR UV-photometer data, the DLR data obtained at pressures between 200 and 180 hPa (the duration time was about 1.6 hours) were averaged and compared with the coincident ILAS measurement at the same pressure levels. Figure 10 shows the corresponding D values obtained from Figures 7, 8, and 9. In general, the ILAS data are in agreement with these reduced vertical resolution remote or in situ sensors within  $\pm 20\%$ .

[43] Figure 11a shows average profiles of ozone measured by ILAS and the ALOMAR-DIAL at Andoya, in the same manner as for previous figures. Similarly, a comparison of ILAS with the CNRS-DIAL at Dumont d’Urville is shown in Figure 11b. Since the DIAL data have a vertical sampling better than 1 km, the data is also processed into 1 km geometric height grid in the same way as was done for the ozonesonde data. From Figure 11a, it is confirmed that the ILAS data is in good agreement with the ALOMAR-DIAL data and is within the RSS error at all altitudes

considered here. From Figure 11b, D values around +10% are seen between 16 and 26 km altitude, but this level of D values is comparable to the RSS error. D values exceeding the combined errors occurred above 27 km and sometimes below 15 km. Since the CNRS-DIAL data obtained in the May–June 1997 period had some instrument problems, the DIAL data for altitudes above 30 km were not reliable during that specific period.

#### 4.4. Comparisons by Month

[44] In this subsection, we examined altitudinal or seasonal changes in D values by comparing ILAS data with other satellite and ozonesonde data for different months. We computed the weighted average of D values with regard to N over 5 or 7 points along the vertical (i.e., the average over 5 km below 50 km and over 7 km above 51 km). It is defined as equation (3).

$$D(\text{weighted mean}) = \frac{\sum_j (D_j \times N_j)}{\sum_j N_j} \quad (j = 1 \text{ to } J; J = 5 \text{ or } 7) \quad (3)$$

For ILAS–other satellite comparisons, results of the D values at each layer for periods specified in Table 6 are shown in Figure 12 as a category plot. The weighted average of the RSS errors for each layer, as was done for

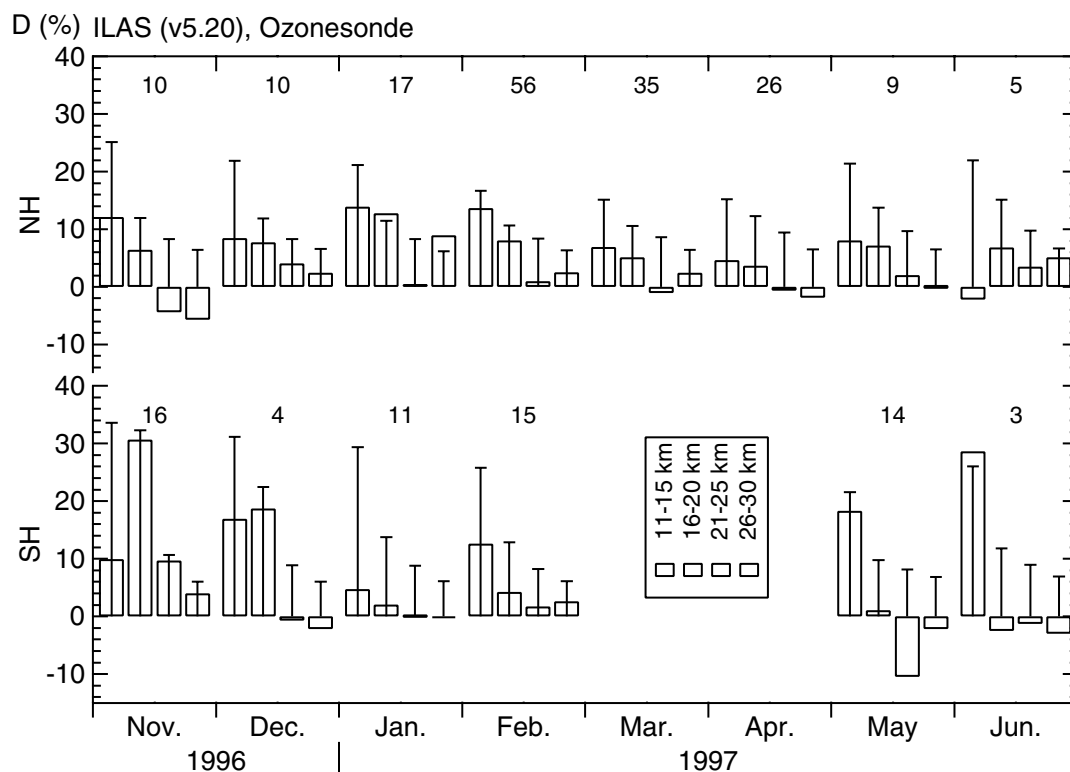


**Figure 13.** Mean relative differences between ILAS and the coincident data of ozonesondes for each 5 km layer. Numbers of coincident measurement profiles are also shown in each subpanel. See color version of this figure at back of this issue.

the D values and defined as equation (4), is also shown as an error bar on the positive side only for better clarity.

$$\text{RSS error (weighted mean)} = \frac{\sum_j N_j (\text{RSSerr}_j \times N_j)}{\sum_j N_j} \quad (4)$$

$(j = 1 \text{ to } J; J = 5 \text{ or } 7)$

where RSSerr is the same as defined in equation (2). For altitudes above 65 km, the errors are quite large so we do not consider these altitudes. The number of coincident measurement profiles specified in Table 6 is given in each subpanel of Figure 12.

[45] Here we summarize these results for different altitude regions separately. Below 20 km (light blue bars), especially in the 11–15 km altitude region, large D values reaching about 50% can be observed. However, the RSS total uncertainty for these altitudes was comparable to the D values, therefore we could not conclude whether any systematic bias in the ILAS ozone data exists or not. Regardless of the validation data, the ILAS ozone data are in good agreement with them in the 21–30 km region (red bars), with relative differences ranging from –5% to 12%. Between 31 and 50 km (green bars), a statistically significant high bias in the ILAS data was generally found from comparisons with the HALOE and SAGE II data for January in the SH. The bias increased with increasing altitude, reaching 18% at the 46–50 km altitude. In the 31–50 km region, however, except for January, the D values remained between –8 and 10%. Between 51 and 64 km (purple bars), there were several cases in which the

D values were higher than the RSS errors, with some D values reaching 18% in these conditions. Otherwise, the D values ranged from –8 to 15%.

[46] For ILAS–ozonesonde comparisons, the averaged D values and RSS errors calculated by equations (3) and (4) at the respective 5 km layers are plotted in Figure 13 for each month and each hemisphere. As seen from the figure, there is no altitudinal or seasonal dependence of the D values in the NH, but higher D values reaching about 30% were seen at the 16–20 km altitude in November and at the 11–15 km altitude in June, both in the SH. Again, these higher D values correspond to an absolute difference as small as 0.2 ppmv.

[47] In summary, there is no significant seasonal dependence of D values in the NH for all altitude regions. However, for the SH, there seems to be some seasonal dependence of D values: the D values are high (30–55%) between 11 and 20 km in November 1996 and exceed the RSS errors between 41 and 57 km in January 1997.

## 5. Discussion and Summary

[48] Discrepancies between the ILAS and the correlative profiles can be caused either by errors in the data compared, or by real atmospheric differences between the sampled air masses. However, if a similar discrepancy is found from comparisons with more than two individual data sources, there is a higher possibility that it is related to issues in the ILAS data. Such phenomena are found from the SH January comparisons both with the HALOE and SAGE II data around 45–55 km altitude where D

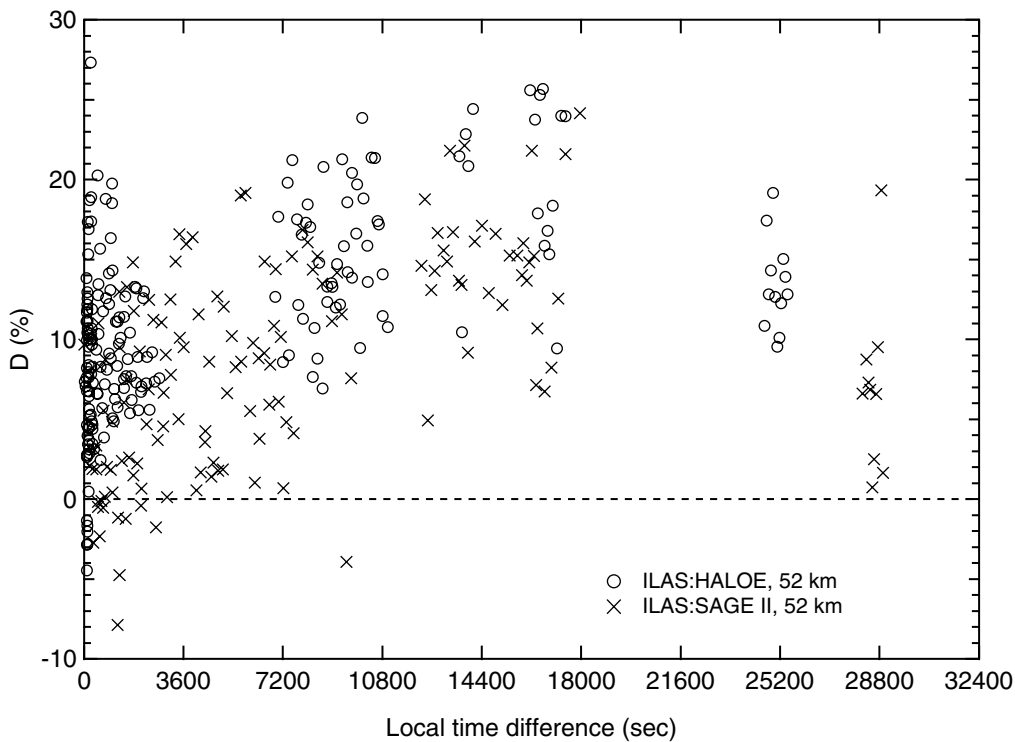


**Figure 14.** Relationship between D value and local time difference for ILAS–HALOE and ILAS–SAGE II at 52 km altitude.

values (relative ILAS–other sensor differences) exceeded the combined measurement errors, and from the SH November comparisons both with the HALOE and POAM II data below 15 km where D values exceeded 40% (see Figure 12). There are several possible causes of these high biases in the ILAS data: uncertainty in the altitude registration, unknown instrument problems, uncertainty in line parameters, and ambiguity in the nongaseous correction method for the effect of aerosol extinction on observed transmittances.

[49] In order to examine the cause of the high bias in the ILAS data for the 45–55 km altitude, the D values were plotted versus the time differences in Figure 14 for ILAS–HALOE and ILAS–SAGE II at the 52 km altitude, as a representative, at which the large D values were found. It is apparent that the magnitude of the D values is related to the local time (LT) difference. A similar feature is also seen even down to 40 km (not shown). On the other hand, although not shown in the figure, the degree of separation in space is insensitive to the D values. Therefore, the cause of the high bias in the ILAS data around 45–55 km is thought to be due to something in the ILAS data related to the LT difference. Further study is required on this issue.

[50] For altitudes below 20 km, no distinct relation between the D value and the local time difference is seen. From the comparisons with data from ozonesonde and balloon-borne, airborne, and ground-based instruments, there are few significant D values exceeding 20% at these altitudes. As we mentioned in section 4, the absolute difference between the ILAS and the correlative data below 15 km is as small as 0.2 ppmv. The high bias in the ILAS

data below 15 km could be related to the altitude registration methods and/or methods used to correct aerosol extinction in the various retrieval algorithms used to process the satellite sensor data. As an example of this type of problem, a detailed discussion on possible differences between altitude registration of POAM II and SAGE II is given by *Randall et al.* [2000]. Although it is necessary to discuss these issues in a comprehensive manner considering validation studies of the other ILAS-retrieved species [e.g., *Kanzawa et al.*, 2002], such a discussion is beyond the scope of this paper. Nevertheless, this is an important issue to be addressed in the near future, but it is also a challenge to retrieve such low ozone mixing ratios at these lower altitudes from satellite. For solar occultation instruments, it is generally difficult to assign the TH accurately, because the Sun as seen from the satellite is significantly distorted owing to atmospheric refraction.

[51] In summary, the relative difference in percentage (D value) ranged from –2 to 11% for the ILAS–HALOE comparisons, from –5 to 9% for the ILAS–SAGE II comparisons, and from –8 to 12% for the ILAS–POAM II comparisons between 21 and 50 km, except for the January SH comparisons at 41–50 km. Between 51 and 64 km, the D values ranged from –8 to 10% for the ILAS–HALOE and ILAS–SAGE II comparisons, although there were some exceptions. The D values ranged from –11 to 10% for the ILAS–ozonesonde comparisons between 21 and 30 km. The D values were within 10% between 13 and 20 km and within 20% at 10–12 km, although they tended to increase with decreasing altitude. The ILAS ozone data also agreed within  $\pm 10\%$  with data from the balloon, aircraft, and ground-based instruments between 9 and 50 km, although

there were some exceptions. This validation study demonstrated that the version 5.20 ILAS ozone data is improved upon version 3.10 ILAS ozone data, which was already shown to be within 13–20% of the HALOE data [Lee et al., 1999] and within 20% of the ozonesonde data [Sasano et al., 1999a]. The overall good agreement between the ILAS and the correlative data used here strongly suggests that the version 5.20 ILAS ozone data can be used reliably and can provide useful information for studies in stratospheric chemistry and dynamics in the high latitudes [e.g., Terao et al., 2002]. Although the routine operation period of ILAS was only 8 months (from November 1996 to June 1997), the ILAS data can be used to derive the ozone trend in the high latitude stratosphere by combining ILAS with POAM II (from 1993 to November 1996), POAM III (from 1998), and scheduled ILAS II (from 2002) [Sasano et al., 2001] sensors.

[52] **Acknowledgments.** We are grateful for the excellent collaboration with the Centre National d'Etude Spatiales (CNES) and the National Scientific Balloon Facility launching teams during the balloon launch operations at Esrange and Fairbanks, respectively. The version 19 HALOE data (processed at the NASA Langley Research Center and the NASA Langley Chemistry and Dynamics Branch), version 6 SAGE II data (processed at the NASA Langley Research Center and the NASA Langley Radiation and Aerosols Branch), and version 6 POAM II data (processed at the Naval Research Laboratory) were obtained publicly through their respective World Wide Web sites (HALOE: <http://haloedata.larc.nasa.gov>; SAGE II: <http://www-sage2.larc.nasa.gov>; POAM II: <http://wvms.nrl.navy.mil/POAM/>). The OSDOC data were supplied by the NADIR team at the Norwegian Institute for Air Research, NILU, Norway. The authors would like to thank the respective Principal Investigators (and institutes) for the OSDOC ozonesonde data: Bojan R. Bojkov (NILU) for the data at Andoya, Gardermoen, and Orland, Manuel Gil (Instituto Nacional de Técnica Aeroespacial (INTA), Spain, and Icelandic Meteorological Office (IMO), Iceland) for the data at Keflavik, Esko Kyro (Finnish Meteorological Institute (FMI), Finland) for the data at Jokioinen and Sodankyla, Ib Steen Mikkelsen (Danish Meteorological Institute (DMI), Denmark) for the data at Scoresbysund and Sondrestrom, Zenobia Litynska (Institute of Meteorology and Water Management (IMWM), Poland) for the data at Legionowo, and Mike Molyneux (United Kingdom Meteorological Office (UKMO), UK) for the data at Lerwick. The ILAS CMDB data were supplied by the Data Handling Facility (DHF) at NIES, Japan. The ALOMAR-DIAL (Georg Hansen, Principal Investigator, of NILU) data used in this publication were obtained as part of the Network for the Detection of Stratospheric Change (NDSC) and is publicly available (<http://www.ndsc.ncep.noaa.gov>). The ozonesonde data at Fairbanks (Bryan Johnson, Holger Vömel, and Samuel Oltmans, Principal Investigators, of National Oceanic and Atmospheric Administration (NOAA)) were obtained through the Photochemistry of Ozone Loss in the Arctic Region in Summer (POLARIS) aircraft campaign database at the Earth Science Division Project Office/NASA Ames Research Center (<http://cloud1.arc.nasa.gov>). The ILAS project has been funded by the Environmental Agency of Japan, to which the authors are greatly obliged.

## References

- Bevilacqua, R. M., Introduction to special section: Polar Ozone and Aerosol Measurement (POAM II), *J. Geophys. Res.*, **102**, 23,591–23,592, 1997.
- Bhatt, P. P., et al., An evaluation of the quality of Halogen Occultation Experiment ozone profiles in the lower stratosphere, *J. Geophys. Res.*, **104**, 9261–9276, 1999.
- Brühl, C., et al., Halogen Occultation Experiment ozone channel validation, *J. Geophys. Res.*, **101**, 10,217–10,240, 1996.
- Brühl, C., P. J. Crutzen, and J. U. Groß, High-latitude, summertime NO<sub>x</sub> activation and seasonal ozone decline in the lower stratosphere: Model calculations based on observations by HALOE on UARS, *J. Geophys. Res.*, **103**, 3587–3597, 1998.
- Camy-Peyret, C., et al., Stratospheric N<sub>2</sub>O<sub>5</sub>, CH<sub>4</sub>, and N<sub>2</sub>O profiles from IR solar occultation spectra, *J. Atmos. Chem.*, **16**, 31–40, 1993.
- Cunnold, D. M., et al., Validation of SAGE II ozone measurements, *J. Geophys. Res.*, **94**, 8447–8460, 1989.
- Cunnold, D. M., et al., SAGE (version 5.96) ozone trends in the lower stratosphere, *J. Geophys. Res.*, **105**, 4445–4458, 2000.
- de Valk, J. P. J. M. M., et al., Airborne heterodyne measurements of stratospheric ClO, HCl, O<sub>3</sub>, and N<sub>2</sub>O during SESAME 1 over northern Europe, *J. Geophys. Res.*, **102**, 1391–1398, 1997.
- Deniel, C., et al., A comparative study of POAM II and electrochemical concentration cell ozonesonde measurements obtained over northern Europe, *J. Geophys. Res.*, **102**, 23,629–23,642, 1997.
- Ferlemann, F., et al., Differential optical absorption spectroscopy instrument for stratospheric balloonborne trace-gas studies, *Appl. Opt.*, **39**, 2377–2386, 2000.
- Fukunishi, H., S. Okano, M. Taguchi, and T. Ohnuma, Laser heterodyne spectrometer using a liquid nitrogen cooled tunable diode laser for remote measurements of atmospheric O<sub>3</sub> and N<sub>2</sub>O, *Appl. Opt.*, **29**, 2722–2728, 1990.
- Glaccum, W., et al., The Polar Ozone and Aerosol Measurement instrument, *J. Geophys. Res.*, **101**, 14,479–14,488, 1996.
- Godin, S., et al., Study of the interannual ozone loss and the permeability of the Antarctic polar vortex from aerosol and ozone lidar measurements in Dumont d'Urville (66.4°S, 140°E), *J. Geophys. Res.*, **106**, 1311–1330, 2001.
- Hansen, G., and M. P. Chipperfield, Ozone depletion at the edge of the Arctic polar vortex 1996/1997, *J. Geophys. Res.*, **104**, 1837–1846, 1999.
- Hofmann, D. J., and S. Solomon, Ozone destruction through heterogeneous chemistry following the eruption of El Chichon, *J. Geophys. Res.*, **94**, 5029–5041, 1989.
- Hoppel, K. W., K. P. Bowman, and R. M. Bevilacqua, Northern Hemisphere summer ozone variability observed by POAM II, *Geophys. Res. Lett.*, **26**, 827–830, 1999.
- Johnson, D. G., K. W. Jucks, W. A. Traub, and K. V. Chance, Smithsonian stratospheric far-infrared spectrometer and data reduction system, *J. Geophys. Res.*, **100**, 3091–3106, 1995.
- Jucks, K. W., et al., Observations of OH, HO<sub>2</sub>, H<sub>2</sub>O, and O<sub>3</sub> in the upper stratosphere: Implications for HO<sub>x</sub> photochemistry, *Geophys. Res. Lett.*, **25**, 3935–3938, 1998.
- Kanzawa, H., C. Camy-Peyret, Y. Kondo, and N. Papineau, Implementation and first scientific results of the ILAS validation balloon campaign at Kiruna–Esrange in February–March 1997, in *Proceedings of the 13th ESA Symposium, European Rocket and Balloon Programmes and Related Research*, pp. 211–215, ESA Publ., Noordwijk, Netherlands, Oland, Sweden, 1997.
- Kanzawa, H., et al., Validation and data characteristics of water vapor profiles observed by the Improved Limb Atmospheric Spectrometer (ILAS) and processed with the Version 5.20 algorithm, *J. Geophys. Res.*, doi:10.1029/2001JD000881, in press, 2002.
- Komhyr, W. D., Electrochemical concentration cells for gas analysis, *Ann. Geophys.*, **25**, 203–210, 1969.
- Komhyr, W. D., et al., Electrochemical concentration cell ozonesonde performance evaluation during STOIC 1989, *J. Geophys. Res.*, **100**, 9231–9244, 1995.
- Lee, K.-M., et al., Intercomparison of ILAS and HALOE ozone at high latitudes, *Geophys. Res. Lett.*, **26**, 835–838, 1999.
- Lu, J., et al., Intercomparison of stratospheric ozone profiles obtained by Stratospheric Aerosol and Gas Experiment II, Halogen Occultation Experiment, and ozonesondes in 1994–1995, *J. Geophys. Res.*, **102**, 16,137–16,144, 1997.
- Lu, C. H., et al., Lagrangian approach for Stratospheric Aerosol and Gas Experiment (SAGE) II profile intercomparisons, *J. Geophys. Res.*, **105**, 4563–4572, 2000.
- Lucke, R. L., et al., The Polar Ozone and Aerosol Measurement (POAM) III instrument and early validation results, *J. Geophys. Res.*, **104**, 18,785–18,799, 1999.
- Lumpe, J. D., et al., POAM II retrieval algorithm and error analysis, *J. Geophys. Res.*, **102**, 23,593–23,614, 1997.
- Manney, G. L., et al., Comparison of satellite ozone observations in coincident air masses in early November 1994, *J. Geophys. Res.*, **106**, 9923–9943, 2001.
- Mauldin, L. E., III, et al., Stratospheric Aerosol and Gas Experiment II instrument: A functional description, *Opt. Eng.*, **24**, 307–312, 1985.
- Morris, G. A., J. F. Gleason, J. Ziemke, and M. R. Schoeberl, Trajectory mapping: A tool for validation of trace gas observation, *J. Geophys. Res.*, **105**, 17,875–17,894, 2000.
- Nakajima, H., et al., Characteristics and performance of the Improved Limb Atmospheric Spectrometer (ILAS) in orbit, *J. Geophys. Res.*, doi:10.1029/2001JD001439, in press, 2002a.
- Nakajima, H., et al., Tangent height registration for the solar occultation satellite sensor ILAS: A new technique for Version 5.20 products, *J. Geophys. Res.*, doi:10.1029/2001JD000607, in press, 2002b.
- NOAA, *Northern Hemisphere Winter Summary 1999–2000*, National Weather Service/National Centers for Environmental Prediction/Climate Prediction Center, 2000a.
- NOAA, *Southern Hemisphere Winter Summary 2000*, National Weather

- Service/National Centers for Environmental Prediction/Climate Prediction Center, 2000b.
- Park, J. H., and J. M. Russell III, Summer polar chemistry observations in the stratosphere made by HALOE, *J. Atmos. Sci.*, *51*, 2903–2913, 1994.
- Pommereau, J.-P., and J. Piquard, Ozone and nitrogen dioxide vertical distributions by UV-visible solar occultation from balloons, *Geophys. Res. Lett.*, *21*, 1227–1230, 1994.
- Proffitt, M. H., and R. J. McLaughlin, Fast-response dual-beam UV absorption ozone photometer suitable for use on stratospheric balloons, *Rev. Sci. Instrum.*, *54*, 1719–1728, 1983.
- Randall, C. E., et al., Comparison of Polar Ozone and Aerosol Measurement (POAM) II and Stratospheric Aerosol and Gas Experiment (SAGE) II aerosol measurements from 1994 to 1996, *J. Geophys. Res.*, *105*, 3929–3942, 2000.
- Randel, W. J., et al., Trends in the vertical distribution of ozone, *Science*, *285*, 1689–1692, 1999.
- Renard, J.-B., et al., Nocturnal vertical distribution of stratospheric O<sub>3</sub>, NO<sub>2</sub> and NO<sub>3</sub> from balloon measurements, *J. Geophys. Res.*, *101*, 28,793–28,804, 1996.
- Russell, J. M., III, The halogen occultation experiment, *J. Geophys. Res.*, *98*, 10,777–10,797, 1993.
- Sasano, Y., et al., Validation of ILAS Version 3.10 ozone with ozonesonde measurements, *Geophys. Res. Lett.*, *26*, 831–834, 1999a.
- Sasano, Y., M. Suzuki, T. Yokota, and H. Kanzawa, Improved limb atmospheric spectrometer (ILAS) for stratospheric ozone layer measurements by solar occultation technique, *Geophys. Res. Lett.*, *26*, 197–200, 1999b.
- Sasano, Y., et al., ILAS-II instrument and data processing system for stratospheric ozone layer monitoring, in *Optical Remote Sensing of the Atmosphere and Clouds II*, edited by Y. Sasano, J. Wang, and T. Hayasaka, *Proc. SPIE Int. Soc. Opt. Eng.*, *4150*, 106–114, 2001.
- Schlager, H., et al., In situ observations of air traffic emission signatures in the North Atlantic flight corridor, *J. Geophys. Res.*, *102*, 10,739–10,750, 1997.
- Schulz, A., et al., Match observations in the Arctic winter 1996/97: High stratospheric ozone loss rates correlate with low temperatures deep inside the polar vortex, *Geophys. Res. Lett.*, *27*, 205–208, 2000.
- Shine, K. P., and P. M. d. F. Forster, The effect of human activity on radiative forcing of climate change: A review of recent developments, *Glob. Planet. Change*, *20*, 205–225, 1999.
- Solomon, S., R. R. Garcia, F. S. Rowland, and D. J. Wuebbles, On the depletion of Antarctic ozone, *Nature*, *321*, 755–758, 1986.
- Stachnik, R. A., et al., Submillimeterwave heterodyne measurements of stratospheric ClO, HCl, O<sub>3</sub>, and HO<sub>2</sub>: First results, *Geophys. Res. Lett.*, *19*, 1931–1934, 1992.
- Swinbank, R., and A. O'Neill, A stratosphere–troposphere data assimilation system, *Mon. Weather Rev.*, *122*, 686–702, 1994.
- Tabazadeh, A., et al., Quantifying denitrification and its effect on ozone recovery, *Science*, *288*, 1407–1411, 2000.
- Terao, Y., et al., Stratospheric ozone loss in the 1996/1997 Arctic winter: Evaluation based on multiple trajectory analysis for double-sounded air parcels by ILAS, *J. Geophys. Res.*, doi:10.1029/2001JD000615, in press, 2002.
- Toon, G. C., The JPL MkIV interferometer, *Opt. Photonic News*, *2*, 19–21, 1991.
- Toon, G. C., et al., Comparison of MkIV balloon and ER-2 aircraft measurements of atmospheric trace gases, *J. Geophys. Res.*, *104*, 26,779–26,790, 1999.
- Waibel, A. E., et al., Arctic ozone loss due to denitrification, *Science*, *283*, 2064–2069, 1999.
- Wennberg, P. O., et al., Removal of stratospheric O<sub>3</sub> by radicals: In situ measurements of OH, HO<sub>2</sub>, NO, NO<sub>2</sub>, ClO, and BrO, *Science*, *266*, 398–404, 1994.
- WMO, *Atmospheric Ozone: 1985*, Rep. 16, Global Ozone Research and Monitoring Project, Geneva, 1986.
- WMO, Assessment of trends in the vertical distribution of ozone, *Stratospheric Processes and Their Role in Climate (SPARC)*, Rep. 1, Global Ozone Research and Monitoring Project, Geneva, 1998.
- WMO, *Scientific Assessment of Ozone Depletion: 1998*, Rep. 44, Global Ozone Research and Monitoring Project, Geneva, 1999.
- Yokota, T., et al., Improved Limb Atmospheric Spectrometer (ILAS) data retrieval algorithm for Version 5.20 gas profile products, *J. Geophys. Res.*, doi:10.1029/2001JD000628, in press, 2002.
- H. Bösch, R. Fitzenberger, and K. Pfeilsticker, Institut für Umweltphysik, University of Heidelberg, Heidelberg, Germany.
- H. Bremer, M. von König, and H. Küllmann, Institut für Umweltphysik, University of Bremen, Bremen, Germany.
- C. Camy-Peyret, P. Jeseck, and S. Payan, Laboratoire de Physique Moléculaire et Applications, CNRS, Paris, France.
- T. Deshler, Department of Atmospheric Science, University of Wyoming, Laramie, WY, USA.
- H. Fukunishi and I. Murata, Department of Geophysics, Tohoku University, Sendai, Japan.
- H. Gernandt, Alfred Wegener Institute for Polar and Marine Research, Bremerhaven, Germany.
- S. Godin, F. Goutail, and J.-P. Pommereau, Service d'Aéronomie, CNRS, Paris, France.
- D. G. Johnson, NASA Langley Research Center, Hampton, VA, USA.
- K. Jucks and W. A. Traub, Harvard–Smithsonian Center for Astrophysics, Cambridge, MA, USA.
- H. Kanzawa, H. Nakajima, H. Nakane, Y. Sasano, T. Sugita, and T. Yokota, Ozone Layer Research Project, National Institute for Environmental Studies, 16-2 Onogawa, Tsukuba, Ibaraki, 305-8506, Japan. (tsugita@nies.go.jp)
- Y. Kondo, Research Center for Advanced Science and Technology, University of Tokyo, Tokyo, Japan.
- J. J. Margitan, B. Stachnik, and G. C. Toon, Jet Propulsion Laboratory, California Institute of Technology, Pasadena, CA, USA.
- J.-B. Renard, Laboratoire de Physique et Chimie de l'Environnement, CNRS, Orléans, France.
- H. Schlager, Institut für Physik der Atmosphäre, DLR, Oberpfaffenhofen, Germany.
- K. Shibasaki, Faculty of Letters, Kokugakuin University, Tokyo, Japan.
- V. Yushkov, Central Aerological Observatory, Dolgoprudny, Russia.

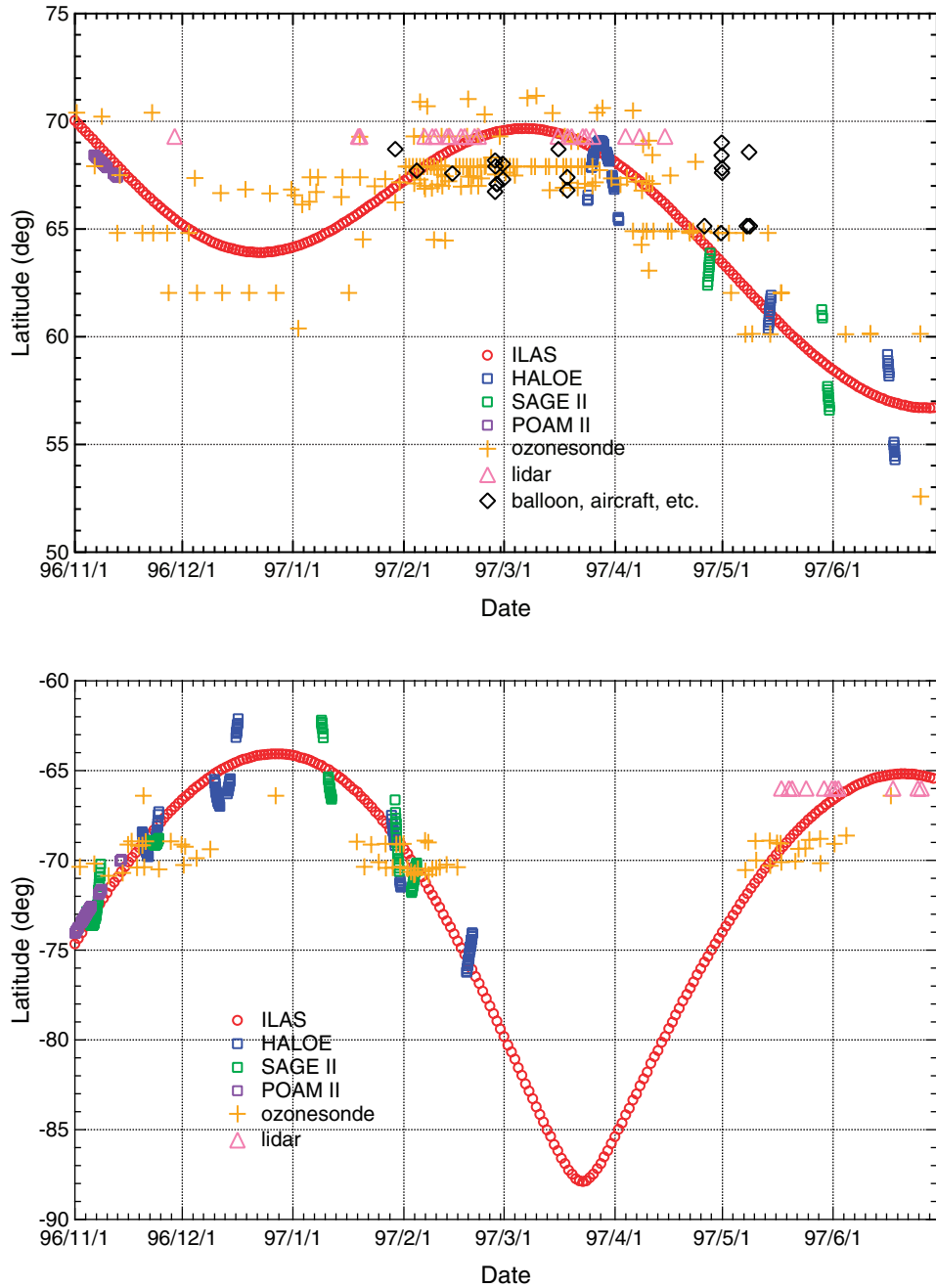


**Figure 1.** Latitudinal coverage of ILAS and the coincident measurements from SAGE II, HALOE, POAM II, ozonesondes, balloon-borne, airborne, and ground-based instruments. The upper panel shows the NH and the bottom panel shows the SH.

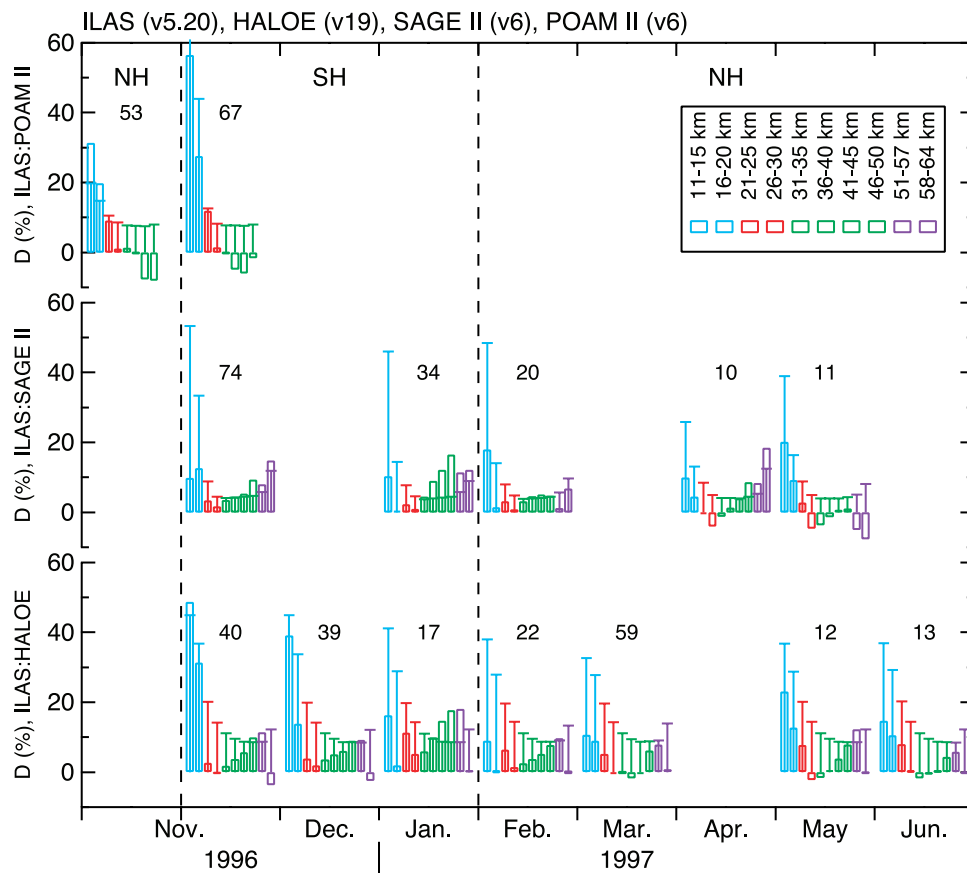


**Figure 12.** Mean relative differences between ILAS and the coincident data of satellite sensors for each 5 or 7 km layer. Numbers of coincident measurement profiles are also shown in each subpanel.

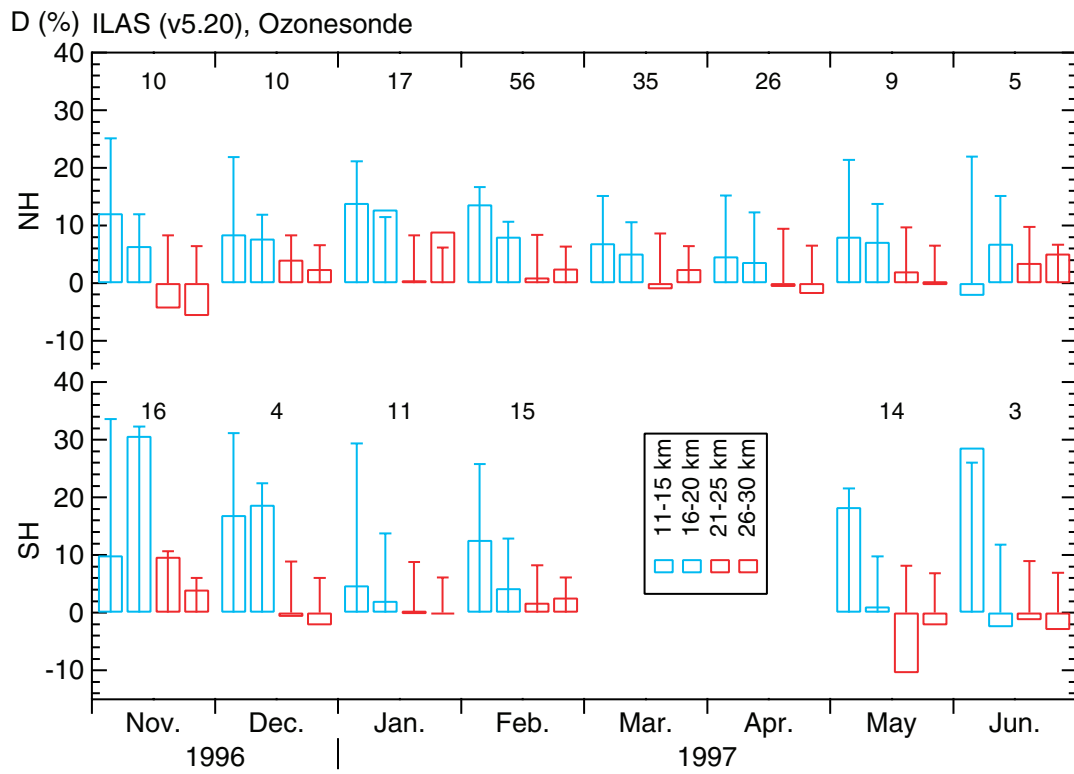


**Figure 13.** Mean relative differences between ILAS and the coincident data of ozonesondes for each 5 km layer. Numbers of coincident measurement profiles are also shown in each subpanel.